hydrophobic "backside" of the molecule containing the D-Tyr[2] and Cys[6] side chains. These side chains impart a net hydrophobic moment to the molecule and may directly enhance binding by shielding the arginine and aspartic acid side-chain interactions with GPIIbIIIa from competition due to solvent. Accordingly, substitution of a hydrophilic residue for D-Tyr[2] results in diminished potency.[20] In kistrin and echistatin, the bulk of the protein may provide a similar shielding function.

Coupling an understanding of the local RGD geometry of **1** with an appropriate placement of hydrophobic groups defines a template for the design of non-peptide antagonists of GPIIb-IIIa-fibrinogen binding. Our construction of that template, and the resulting design efforts, will be reported in the future.

Experimental Section

Synthesis. The synthesis and characterization of compounds **1-3** have been described by Barker.[20] L-Cysteine (95% ^{15}N) was purchased from Cambridge Isotope Laboratories, Woburn, MA.

NMR Measurements. All spectra were recorded on a Varian VXR-300S spectrometer at 293 K unless noted. All samples were 10 mM in water (10% ^2H atoms for amide NH detection, 99.9% ^2H atoms otherwise) and were adjusted to a pH of 6.8-7.0 with sodium bicarbonate or sodium phosphate. Chemical shifts were measured relative to the HOD signal at 4.85 ppm. The pulse sequences used were supplied within the VNMR software (Varian Associates, release 3.2). Deuterium oxide (99.9% ^2H atoms) was purchased from Aldrich.

One-dimensional ^1H NMR spectra: 90° pulse 10.5 μs, pulse width 3.5 μs, 64 acquisitions. The amide temperature coefficient studies were performed at 273-323 K in 2-deg steps from 273 to 293 K and 5-deg steps from 293-323 K. Side-chain resonance coalescence experiments were performed at 293-363 K in 5-deg increments.

COSY spectra: relaxation delay 2 s, 90° pulse 10.5 μs, spectral width in both $f1$ and $f2$ dimensions 3500 Hz.

ROESY spectra: relaxation delay 2 s, 90° pulse 10.5 μs, pulse width for spin-lock field 1.8 μs, mixing time 50 μs, spectral width in both $f1$ and $f2$ dimensions 3500 Hz.

Acknowledgment. We gratefully acknowledge Jeffrey Y. K. Tom, Kathryn S. Chan, and Martin Struble for the synthesis and purification of **1b-3b**. We would also like to acknowledge and thank Gerhard Wagner for invaluable discussions and advice.

Supplementary Material Available: ROESY spectra of **2a** and **3a** in water (99.9% ^2H atoms), ^1H chemical shift tables for **2a** and **3a**, and coordinates for one of the minimized A-1 structures (5 pages). Ordering information is given on any current masthead page.

Toward the Development of Photo *cis*-Platinum Reagents. Reaction of *cis*-Dichlorobis(1,10-phenanthroline)rhodium(III) with Calf Thymus DNA, Nucleotides, and Nucleosides[1]

R. E. Mahnken, M. A. Billadeau, E. P. Nikonowicz, and H. Morrison*

Contribution from the Department of Chemistry, Purdue University, West Lafayette, Indiana 47907. *Received June 22, 1992*

Abstract: Photolysis of the title compound (cisDCBPR) with calf thymus DNA leads to the formation of covalent adducts. The reaction is not dependent on oxygen, proceeds with moderate (ca. 10^{-3}) quantum efficiency, and occurs with modest enantioselectivity which is enhanced in low ionic strength media, where electrostatic and/or intercalatory association is evident. At least two covalent adducts involving deoxyguanosine as a ligand have been isolated from the enzymatic degradation of the metalated DNA, one of which is spectroscopically identical with an adduct prepared from the reaction of cisDCBPR with dG. Extensive spectral characterization of the second dG adduct implicates N1 as the point of attachment of Rh to the base. A stable adduct with dA has also been isolated from photolysis of the metal complex with the nucleoside, and a structure involving binding to N3 is tentatively assigned.

The interaction of transition-metal complexes with DNA is an active area of research, particularly in the development of new biochemical tools and in the design of new drugs.[2-5] Metal complexes have been used as artificial nucleases[5,6] and DNA conformational probes[7-9] and are in clinical use as antitumor agents, as exemplified by the well-known chemotherapeutic agent cisplatin (*cis*-$Pt(NH_3)_2Cl_2$, *cis*-diamminedichloroplatinum(II), cisDDP).[10-14] DNA is a particularly good target for metal complexes as it offers a wide variety of potential metal binding sites. Such sites include the electron-rich DNA bases or phosphate groups that are available for direct covalent coordination to the metal center and offer the possibility of creating both intra- and interstrand cross-links. There are noncovalent binding modes as well, such as hydrogen bonding and electrostatic binding to grooved regions of the DNA and intercalation of planar aromatic ligands into the stacked base pairs. The interactions of transition-metal complexes with DNA are affected by variations in the metal and the metal oxidation state, the nature of the ligands, the stereochemistry of the metal complex, etc.

Because of our general interest in light-activated DNA binding agents[15,16] and the current interest in the development of photo-

(1) Organic Photochemistry. 98. For 97, see: Mohammad, T.; Morrison, H. *Photochem. Photobiol.* **1992**, *5*, 631-638. For 96, see: Wu, Z. Z.; Morrison, H. *J. Am. Chem. Soc.* **1992**, *114*, 4119. Abstracted, in part, from the doctoral dissertation of R.E.M., Purdue University, May 1991.

(2) Martin, R. B.; Mariam, J. H. *Met. Ions. Biol. Syst.* **1979**, *8*, 57-124.

(3) *Metal Ion-Nucleic Acid Interactions*; Spiro, T., Ed.; Wiley: New York, 1980.

(4) *Metal-DNA Chemistry*; Tullius, T. D., Ed.; ACS Symposium Series 402; American Chemical Society: Washington, DC, 1989.

(5) Pyle, A. M.; Long, E. C.; Barton, J. K. *J. Am. Chem. Soc.* **1989**, *111*, 4520-4522. Sitlani, A.; Long, E. C.; Pyle, A. M.; Barton, J. K. *J. Am. Chem. Soc.* **1992**, *114*, 2303-2312.

(6) Basile, L. A.; Barton, J. K. *Met. Ions. Biol. Syst.* **1989**, *25*, 31-103 and references therein.

(7) Barton, J. K. *Science* **1986**, *233*, 727-734. Pyle, A. M.; Barton, J. K. *Prog. Inorg. Chem.: Bioinorg. Chem.* **1990**, *38*, 413-475. See also: Pyle, A. M.; Morii, T.; Barton, J. K. *J. Am. Chem. Soc.* **1990**, *112*, 9432-9434.

(8) Barton, J. K.; Goldberg, J. M.; Kumar, C. V.; Turro, N. J. *J. Am. Chem. Soc.* **1986**, *108*, 2081-2088.

(9) Mei, H.; Barton, J. K. *Proc. Natl. Acad. Sci. U.S.A.* **1988**, *85*, 1339-1343.

(10) Sherman, S. E.; Lippard, S. J. *Chem. Rev.* **1987**, *87*, 1153-1181.

(11) Lippard, S. J. *Acc. Chem. Res.* **1987**, *11*, 211-217.

(12) Reedijk, J.; Fichtinger-Schepman, A. J.; van Oosterom, A. T.; van der Putte, P. *Struct. Bonding* **1987**, *67*, 53-89.

(13) Umapathy, P. *Coord. Chem. Rev.* **1989**, *95*, 129-181.

(14) Sundquist, W. I.; Lippard, S. J. *Coord. Chem. Rev.* **1990**, *100*, 293-322.

0002-7863/92/1514-9253$03.00/0

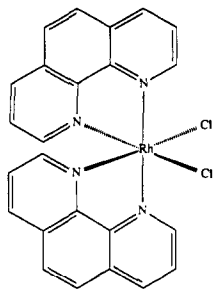

Figure 1. *cis*-Dichlorobis(phenanthroline)rhodium(III), cisDCBPR.

chemotherapeutic reagents,[17-19] we became interested in examining the ability of transition-metal complexes to covalently bind to DNA upon irradiation with UV and visible light. We hoped to elicit chemistry analogous to that exhibited by cisDDP, the antitumor activity of which is believed to be a consequence of the inhibition of DNA replication through the formation of adducts having covalent intrastrand cross-links between neighboring guanosine bases. Such cross-links, with the metal bound to N7 of guanine, are proposed as the major DNA lesions responsible for inhibition of DNA synthesis. The formation of the guanosine adducts is a consequence of cisDDP thermal lability at low chloride concentrations and the resultant formation of aquated species via associative substitution of the chlorides with water. Substitution of both *cis*-aquo ligands by N7 on neighboring guanine bases provide the DNA cross-link.

We chose for our study complexes of the platinum group metal rhodium(III), because the majority of the coordination complexes of this metal ion are known to be thermally inert and photochemically labile.[20,21] The d^6 electron configuration provides a stable oxidation state with the complexes having low spin and pseudooctahedral geometry. The focus of our research was to combine the DNA binding properties characteristic of cisDDP with photochemical activation, thereby creating a reagent that could potentially combine the antitumor effect of cisDDP with site-selective activation.

Our prototype reagent *cis*-$Rh(phen)_2Cl_2^+$ (*cis*-dichlorobis(1,10-phenanthroline)rhodium(III), cisDCBPR)[22] is shown in Figure 1. This complex contains two aromatic 1,10-phenanthroline ligands and two chloride ligands in a cis geometry and is positively charged. The positive charge and phenanthroline ligands provide a means by which the complex could associate with the DNA by electrostatic binding or intercalation, respectively. Due to the helical nature of the two phenanthroline ligands, the complex exists in two enantiomeric forms, thus presenting the potential for enantioselective binding to DNA. cisDCBPR exhibits a long wavelength transition at ca. 380 nm which has been assigned to a metal-centered d–d transition,[23] with other absorption bands at 334 and 351 nm assigned to intraligand transitions. It is reported to undergo substitution of a chloride ligand upon irradiation at 254 and 350 nm.[24] The photosubstitution occurs from the lowest lying, metal-centered d–d triplet excited state (^{3}d–d).[20] The ability of the complex to undergo photoaquation provides a potential mechanism by which other nucleophiles (e.g., electron-rich DNA sites) could directly replace chloride and bind to the metal center or photolytically bind to the rhodium via a chloroaquo intermediate.[25] The cis relationship of the chloride ligands could potentially lead to intrastrand DNA cross-linking analogous to that observed with cisDDP. Finally, the cisDCBPR long wavelength transitions allow selective excitation of the metal complex and avoid potential photochemistry from DNA excited states (λ_{max} 260 nm).

cisCDBPR has been reported to be slightly mutagenic in the dark.[26] Though we know of no phototoxicity studies on this particular complex, it has been reported that irradiation of the analogous bipyridyl complex *cis*-$Rh(bpy)_2Cl_2^+$ increased genotoxicity of DNA repair deficient bacterial cells.[27] The emphasis of our studies has been on the photoinduced *covalent binding* of metal complexes to DNA, and, to our knowledge, there are two relevant reports of the binding of related pseudooctahedral complexes, both in the absence of light. *cis*-$Ru(phen)_2Cl_2$ is reported to covalently bind to DNA with a preference for the Λ enantiomer,[28] and adducts of *trans*-$RuCl_2(DMSO)_4$ with dG have been isolated and identified.[29] There have been more extensive studies of positively charged pseudooctahedral transition-metal complexes with tris(polypyridyl) ligands, such as $M(AA)_3^{n+}$ (M = Ru(II), Rh(III), Co(II), Ni(III); AA = phen, bpy, dip), as photolytic biomolecular conformational probes and DNA cleaving agents.[5,8,30-32] The nuclease activity of these complexes permits the cleavage of DNA with a high sequence specificity. These complexes are photochemically substitutionally inert and therefore only interact with DNA through noncovalent modes. Due to the extensive interest in the area of DNA photocleaving agents, we have not stressed this mode of DNA interaction but have concentrated instead on aspects of covalent binding.[33]

Results

Our studies of the covalent binding of cisDCBPR to DNA were conducted using single- and double-stranded DNA, several wavelengths of light, various time intervals, several ionic strengths, and aerated or deoxygenated solutions. To ensure that the binding was indeed covalent, we subjected all DNA/rhodium photolysis mixtures to exhaustive dialysis and precipitation, with representative samples also subjected to multiple precipitations and Sephadex chromatography. We report the amount of rhodium bound to the DNA as nmol of Rh bound per mg of isolated DNA or as metal bound per DNA base.

A. Photoinduced Reactions of cisDCBPR with Polynucleic Acids. Photolysis of cisDCBPR and Its Diaquo Derivative and Native and Denatured DNA Using Broad-Band Light (λ > 330 nm). Typically these studies involved irradiation of cisDCBPR

(15) Mohammad, T.; Baird, W. M.; Morrison, H. *Bioorg. Chem.* **1991**, *19*, 88–100 and references therein.
(16) For a general review of DNA photochemistry and the photolytic reactions of molecules with DNA, see: *Bioorganic Photochemistry. Photochemistry and the Nucleic Acids*; Morrison, H., Ed.; John Wiley and Sons: New York, 1990; Vol. 1.
(17) For reviews of photodynamic therapy using hematoporphyrin derivatives and visible light, see: Gomer, C. J. *Photochem. Photobiol.* **1991**, *54*, 1093–1107. Henderson, B. W.; Dougherty, T. J. *Ibid.* **1992**, *55*, 145–157.
(18) For a review of the use of psoralens and UVA light, see: Cimino, G. D.; Gamper, H. B.; Isaacs, S. T.; Hearst, J. E. *Ann. Rev. Biochem.* **1985**, *54*, 1151–1193.
(19) Recent developments have allowed for external irradiation of a patient's blood in the presence of a photoactive drug ("photophoresis"), cf. Edelson, R.; Berger, C.; Gasparro, F.; Jegasothy, B.; Heald, P.; Wintroub, B.; Vonderheid, E.; Knobler, R.; Wolff, K.; Plecvig, G.; McKiernan, G.; Christiansen, I.; Oster, M.; Honigsmann, H.; Wilford, H.; Kokoschka, R.; Rehle, T.; Perez, M.; Stingl, G.; Laroche, L. *New Eng. J. Med.* **1987**, *316*, 297–303.
(20) Ford, P. C.; Wink, D.; Dibenedetto, J. *Prog. Inorg. Chem.* **1983**, *30*, 213–271.
(21) Ford, P. C. *J. Chem. Ed.* **1983**, *60*, 829–833.
(22) Gidney, P. M.; Gillard, R. D.; Heaton, B. T. *J. Chem. Soc., Dalton Trans.* **1972**, 2621–2628.
(23) McKenzie, E. D.; Plowman, R. A. *J. Inorg. Nucl. Chem.* **1970**, *32*, 199–212.
(24) Muir, M. M.; Huang, W.-L. *Inorg. Chem.* **1973**, *12*, 1831–1835. For a recent review of rhodium(III) amine complex photochemistry and photophysics, see: Skibsted, L. H. *Coord. Chem. Rev.* **1989**, *94*, 151–179.
(25) Endicott, J. F.; Ramasami, T.; Tamilarasan, R.; Lessard, R. B.; Kul Ryu, C.; Brubaker, G. R. *Coord. Chem. Rev.* **1987**, *77*, 1–87.
(26) Warren, G.; Abbott, E.; Schultz, P.; Bennett, K.; Rogers, S. *Mutat. Res.* **1981**, *88*, 165–173.
(27) Lavelle, J. M.; Krause, R. A. *Mutat. Res.* **1986**, *172*, 211–222.
(28) Barton, J. K.; Lolis, E. *J. Am. Chem. Soc.* **1985**, *107*, 708–709. Danishefsky, A. Ph.D. Dissertation, Columbia University, 1987. Grover, N.; Gupta, N.; Thorp, H. H. *J. Am. Chem. Soc.* **1992**, *114*, 3390–3393.
(29) Cauci, S.; Viglino, P.; Esposito, G.; Quadrifoglio, F. *J. Inorg. Biochem.* **1991**, *43*, 739–751.
(30) (a) Barton, J. K.; Raphael, A. L. *Proc. Natl. Acad. Sci. U.S.A.* **1985**, *82*, 6460–6464. (b) Barton, J. K. *Science* **1986**, *233*, 727–734. (c) Mei, H.; Barton, J. K. *Proc. Natl. Acad. Sci. U.S.A.* **1988**, *85*, 1339–1343. (d) Kirshenbaum, M. R.; Tribolet, R.; Barton, J. K. *Nucleic Acids Res.* **1988**, *16*, 7943–7960.
(31) Stradowski, C.; Gorner, H.; Currell, L. J.; Schulte-Frohlinde, D. *Biopolymers* **1987**, *26*, 189–201.
(32) (a) Kelly, J. M.; Tossi, A. B.; McConnell, D. J.; OhUigin, C. *Nucleic Acids Res.* **1985**, *13*, 6017–6034. (b) Tossi, A. B.; Kelly, J. M. *Photochem. Photobiol.* **1989**, *49*, 545–556.
(33) For a preliminary communication, see: Mahnken, R. E.; Bina, M.; Deibel, R. M.; Morrison, H. *Photochem. Photobiol.* **1989**, *49*, 519–522.

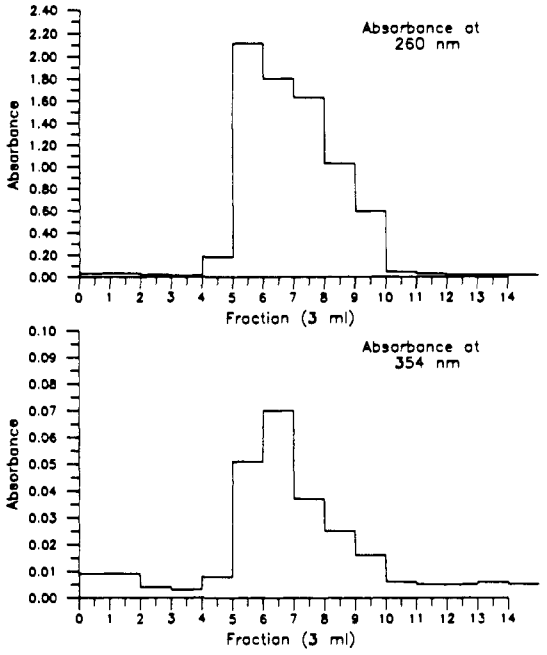

Figure 2. Sephadex chromatogram of native DNA containing covalently bound rhodium complex.

with DNA in non-deoxygenated solutions using a 450-W medium pressure mercury lamp surrounded by a uranium yellow glass filter. The complex (1 mL, 2 mM) was mixed with native or heat-denatured calf thymus DNA (1 mL, 3 mg/mL; DNA(P):cDCBPR = 4.5:1) in a 0.1 M phosphate buffer (pH 6.9) and photolyzed for 2 h. After photolysis the samples were subjected to a standard procedure of exhaustive dialysis and precipitation. The native and denatured DNA/cisDCBPR reaction mixtures, when photolyzed, undergo a visible color change, from pale yellow to dark yellow. After dialysis and precipitation the DNA retains a noticeably yellow color. The electronic absorption spectrum of the isolated DNA shows the characteristic transitions of cisDCBPR (and its monoaquo complex cisMABPR) at 334 and 351 nm, with some enhancement of the long wavelength tail at 380–400 nm. Binding levels of 131 ± 7 (average of 5 runs) and 317 ± 12 (average of 3 runs) nmol of rhodium/mg DNA were observed for native and denatured nucleic acid, respectively. No binding was observed in the absence of light.

In separate experiments native DNA was isolated after photolysis with cisDCBPR and precipitated without dialysis. The DNA was examined by circular dichroism and found to exhibit an increase in the ellipticity normally observed at +275 nm ($\Delta\epsilon_{275nm}$ for DNA ca. 2.5 M^{-1} cm^{-1}). The increase is more pronounced at higher levels of metal binding, and there is a clear shift of the band toward shorter wavelength. Though the cisDCBPR and its photoproducts also show Cotton effects in this region, a shift to longer wavelength would be expected (the Λ isomer of cisDCBPR is reported to have $\Delta\epsilon$ of +94 M^{-1} cm^{-1} at 279 nm).[22]

The metal complex was also photolyzed for 2 h in the absence of DNA, and the photoproducts then reacted with both native and denatured DNA in the dark; no binding of rhodium to the nucleic acid was observed.

In order to firmly establish that the binding of rhodium to DNA was indeed covalent, a sample of native DNA which had been photolyzed with cisDCBPR in the presence of air and then exhaustively dialyzed and precipitated was subjected to size exclusion chromatography. The eluent was monitored by UV spectroscopy at 260 and 354 nm; the results are presented in Figure 2 and demonstrate the coelution of the DNA and the rhodium complex. Control studies show the cisDCBPR elutes in fractions 13–17 under these chromatographic conditions.

A time course study was carried out with native calf thymus DNA (1 mL, 2.3 mg/mL) and cisDCBPR (1 mL, 1.7 mM). Six samples were photolyzed over a range of 14 h in air. The solutions were each analyzed by HPLC for remaining starting material and

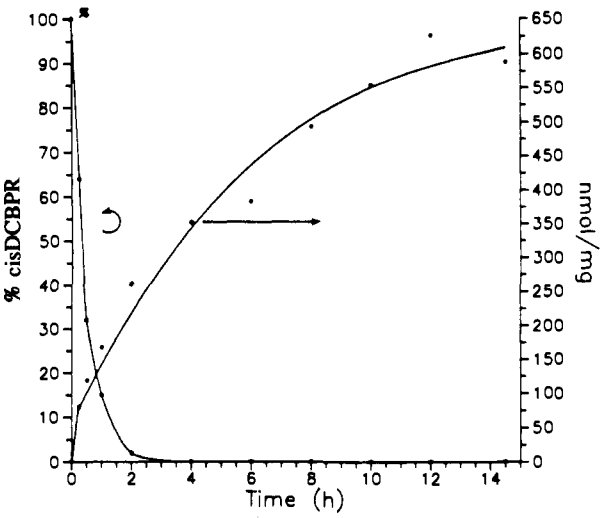

Figure 3. Time course study for photolysis of cisDCBPR with native DNA.

Table I. Comparative Photolysis of cisDCBPR and cisDABPR with Native and Denatured DNA[a]

	cisDCBPR nmol/mg (metal/base)[b]	cisDABPR nmol/mg (metal/base)[b]
native	116 ± 6 (0.038 ± 0.0023)	107 ± 6 (0.035 ± 0.0023)
denatured	337 ± 8 (0.11 ± 0.0026)	242 ± 8 (0.080 ± 0.0026)

[a] Samples irradiated 125 min in 0.1 M phosphate buffer, pH 7 DNA:cisDCBPR ratio = 3:1. [b] Data are averages of duplicate runs.

Table II. Covalent Binding Values for the Irradiation of cisDCBPR with Native and Denatured DNA at Four Ionic Strengths[a]

	nmol/mg (metal/base)	
ionic strength	native DNA	denatured DNA
0.083	369 (0.12)	595 (0.20)
0.041	448 (0.15)	694 (0.23)
0.021	580 (0.19)	782 (0.26)
0.010	601 (0.20)	810 (0.27)

[a] Samples irradiated for 154 min at DNA(P):cDCBPR ratio = 3:1.

for rhodium bound to isolated and purified DNA. The results are shown in Figure 3. It is clear that the binding level increases well after all the cisDCBPR has been consumed, with a plateau at ca. 580 nmol/mg, a degree of incorporation corresponding to 1 metal atom per 5 DNA bases. At this point, ca. 50% of the complex has become covalently bound to the DNA. Though samples irradiated beyond 4 h gave DNA which appeared to be more denatured (powdery rather than globular), there was no significant change in the amount of DNA isolable over the full 14 h of the photolysis. A 12-h dark control gave no evidence for binding of rhodium to the DNA.

Since the time course study gives clear evidence that photoproducts of cisDCBPR are also capable of photolytically binding to DNA, comparative studies with the diaquo complex *cis*-Rh(phen)$_2$(H$_2$O)$_2^{3+}$ (cisDABPR) were carried out under the standard photolytic conditions. The data are presented in Table I and confirm that this photoproduct is also capable of being photolytically bound to DNA.[34]

Our standard photolysis experiments were carried out in a 0.1 M phosphate buffer (pH 7), corresponding to an ionic strength $I = 0.22$. The potential role of ionic strength on photolytic binding was examined by irradiating cisDCBPR (1 mL, 2 mM) with native and denatured DNA (1 mL, 2 mg/mL) in phosphate buffer

(34) cisDCBPR is thermolytically hydrolyzed to mono- and bisaquo products as evidenced by HPLC analysis. One would therefore expect that photolysis of a thermolysis product mixture with DNA would lead to incorporation of the metal. We have confirmed that such is indeed the case, using a reaction mixture resulting from refluxing cisDCBPR for 46 h in 0.1 M phosphate buffer (pH 7.2). No binding of the thermolysis products is observed in the absence of light.

Table III. Binding of cisDCBPR with Polyribonucleotides Using Broad-Band Light[a]

	nmol/mg	metal/base
Poly G	265 ± 11	0.087 ± 0.004
Poly A	167 ± 3	0.055 ± 0.001
Poly U	68 ± 19	0.023 ± 0.007
Poly C	12 ± 2	0.0039 ± 0.0006

[a] Samples irradiated 2 h in 0.01 M phosphate buffer, pH 7, in aerated solutions. Data are averages of duplicate runs.

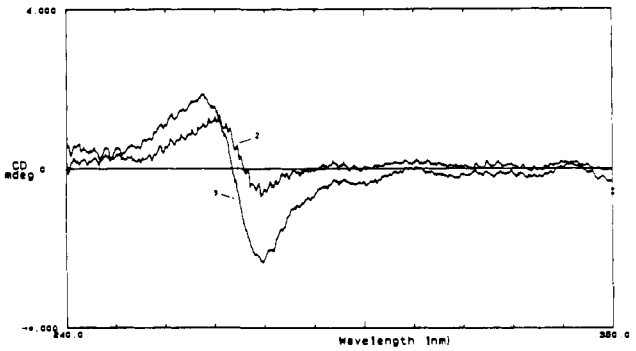

Figure 4. CD spectra of metal complexes recovered after photolysis of native DNA with cisDCBPR: 1 = cisDCBPR, 2 = cisMABPR.

solutions with I = 0.08, 0.04, 0.02, and 0.01. The results are presented in Table II and indicate that higher levels of binding correlate with decreasing ionic strength.

Photolysis of cisDCBPR with Polyribonucleotides. cisDCBPR was irradiated with each of the four single stranded polyribonucleotides in order to test for potential base specificity in the DNA photometalation reaction. Duplicate samples of Poly C, Poly U, Poly A, and Poly G (1 mL, 2.6–2.7 mg/mL) were irradiated with the complex (1 mL, 1.9 mM) in a 0.01 M phosphate buffer (pH 7) for 120 min using the standard photolysis conditions. After irradiation, the samples were dialyzed, precipitated, and analyzed as above. The binding values are shown in Table III.

Enantioselectivity of the cisDCBPR Photoreaction with DNA. Native calf thymus DNA (0.5 mL, 0.82 mg/mL) was photolyzed with cisDCBPR (0.5 mL, 0.65 mM) in aerated and deoxygenated 0.1 M phosphate buffer (pH 7) solutions for 100 min. cisDABPR (0.5 mL, 0.83 mM) was photolyzed with DNA in a concomitant experiment. The DNA was precipitated and the supernatants were examined for optical activity by CD. The solutions exhibited negative Cotton effects at 279 nm, which can be attributed to enrichment in the Δ isomers if one assumes that the aquated metal complex photoproducts have CD characteristics analogous to those of cisDCBPR (for which $\Delta\epsilon_{279nm}$ = +94 M^{-1} cm^{-1} for the D (Λ) isomer).[22]

In a second experiment, native DNA (1 mL, 3.5 mg/mL) was photolyzed with cisDCBPR (1 mL, 2 mM) for 62 min using the standard photolysis conditions. After precipitation of the DNA the major products were collected by HPLC and examined for optical activity. The CD spectra are presented in Figure 4 and show that both the recovered cisDCBPR and its monoaquo product cisMABPR give negative Cotton effects at 279 nm, consistent with enrichment of the Δ isomers.

In order to better quantitate the amount of optical enrichment, cisDCBPR (0.5 mL, 2.8 mM) was irradiated with native DNA (0.5 mL, 4 mg/mL) under standard conditions for 30, 60, and 120 min. The DNA was immediately precipitated after photolysis and analyzed for bound rhodium while the supernatants were examined for optical activity by CD. The data are given in Table IV and indicate that increased levels of covalent binding of rhodium are associated with modest increases in enantiomeric excess (ee).

Photolysis with Monochromatic Light. Quantum Efficiencies for Covalent Binding of cisDCBPR and cisDABPR to DNA. Quantum efficiencies for photoinduced rhodium incorporation into native and denatured calf thymus DNA were determined in both normal and argon-deoxygenated solutions using 308-nm light. The

Table IV. Photolytic Incorporation of Rhodium and Enantioselectivity upon Photolysis of cisDCBPR with Native DNA

phot time (min)	nmol/mg	nmol bound	$\Delta\epsilon$[a]	% ee[b]	binding ratio (Λ/Δ)[c]
0	0	0			
30	113	282	3.0	3.2	1.07
60	118	307	3.4	3.6	1.07
90	162	422	5.5	5.8	1.13
120	208	437	6.4	6.8	1.15

[a] $\Delta\epsilon_{279\,nm}$ in the supernatant; $\Delta\epsilon$ = {[deg/concentration (M) × cell length (cm)] × 100}/3300. [b] % ee = $\Delta\epsilon$ in supernatant/94 M^{-1} cm^{-1} (based on +94 M^{-1} cm^{-1} for the Λ isomer of cisDCBPR).[22] [c] Ratio of nmol of Λ bound to nmol of Δ bound. Λ = X + [(nmol bound − X)/2] where X = (nmol bound) × % ee. Δ = nmol bound − Λ.

Table V. Quantum Efficiencies for the Photometalation of Native and Denatured DNA with cisDCBPR and cisDABPR[a]

	DNA isolated (mg)	Φ (×10^{-3})
cisDCBPR/native DNA		
air	2.6	1.1
argon	2.1	0.91
cisDCBPR/denatured DNA		
air	2.4	5.9
argon	2.7	6.9
cisDABPR/native DNA		
air	2.3	0.88
argon	2.4	0.91
cisDABPR/denatured DNA		
air	2.7	2.2
argon	2.2	2.1

[a] Samples in 0.1 M phosphate buffer, pH 7. Irradiation with a XeCl excimer laser emitting at 308 nm at an average laser power = 4.9 mJ/pulse (2.12 × 10^{17} photons/s) for 4 min. DNA(P):metal complex ratio = 4.7:1.

photolyses were conducted using 1 cm^2 of a 2.6- × 1-cm beam from a XeCl excimer laser operating at 5 mJ/pulse. DNA (1.5 mL, 2.0 mg/mL) and cisDCBPR or cisDABPR (1.5 mL, 1.3 mM) were photolyzed for 4 min. The argon-deoxygenated samples were bubbled with argon for 30 min. HPLC analysis of the cisDCBPR reaction mixture showed that the amount of starting material remaining after photolysis was ca. 60–70%. (The major photoproduct was the monoaquo complex; a small amount of cisDABPR was formed.) The data are presented in Table V.

B. Interaction of cisDCBPR with DNA in the Absence of Light. Noncovalent binding (e.g., association) of the metal complex to DNA was investigated using classical equilibrium dialysis experiments (including circular dichroism spectropolarimetry), electronic absorption spectroscopy, and DNA melting transitions.

Equilibrium Dialysis Studies. Initial dialysis studies were carried out under the conditions used in the photolysis reactions (i.e., with 0.1 M phosphate buffer but with lower concentrations of the DNA and metal complex) and gave no evidence of deviation from equilibrium. The concentration of the metal complex was determined either by UV spectroscopy, in which case the concentration of cisDCBPR outside the dialysis bag was compared with control samples containing only the rhodium complex, or by atomic absorption, in which case the amount of the metal complex was measured inside and outside the dialysis bag after acid hydrolysis of the DNA. Further studies examined association as a function of ionic strength, with concomitant experiments using other metal pseudooctahedral complexes (cisDABPR, $Rh(phen)_3^{3+}$ (TPRh), *cis*-$Rh(bpy)_2Cl_2^+$ (cisDCBBR), and $Ru(phen)_3^{2+}$ (TPRu)) for purposes of reference. Typically, DNA (2 mL, 0.46–0.53 mg/mL, 1.6 mM) was dialyzed against the complex (2 mL, 0.35 mM) for 36–48 h in buffer solutions containing 100 mM, 10 mM, and 1 mM phosphate at pH 7 with 2 mM NaCl. The amount of metal complex in the dialysate was determined by comparing the concentration outside the bag with the concentration of control samples run in the absence of DNA. In the case of cisDCBPR, two samples were assayed at each ionic strength, and a detailed analysis of these experiments is shown in Table VI. Included in this table are intrinsic binding constants, calculated using a

Table VI. Noncovalent Association of cisDCBPR with DNA in the Dark as a Function of Ionic Strength[a]

ionic strength	nmol assoc with DNA	% assoc[b]	metal/base	K M^{-1}
0.22	0	0	0	0
0.022	66 ± 22	11 ± 4	0.039 ± 0.013	1.5×10^2
0.0042	126 ± 14	26 ± 3	0.077 ± 0.007	4.3×10^2

	$\Delta\epsilon_{279\ nm}$	% ee[c]	Λ bound/Δ bound
0.22			
0.022	−5.2 ± 0.9	5.5 ± 0.5	1.12 ± 0.01
0.0042	−10.9 ± 1.6	11.5 ± 1.5	1.26 ± 0.04

[a] All solutions at pH 7: I = 0.22, 100 mM PB; I = 0.022, 10 mM PB; I = 0.0042, 1 mM PB and 2 mM NaCl. Data are the average of duplicate experiments. [b] % assoc = nmol assoc/total nmol in solution. [c] % ee = $(\Delta\epsilon_{observed}/\Delta\epsilon_{maximum})100$.

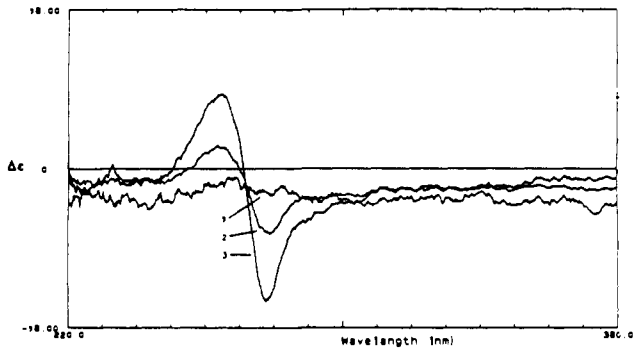

Figure 5. CD spectra for the dialysate from dialysis of cisCDBPR against native DNA at three ionic strengths: 1, I = 0.22; 2, I = 0.022; 3, I = 0.0042.

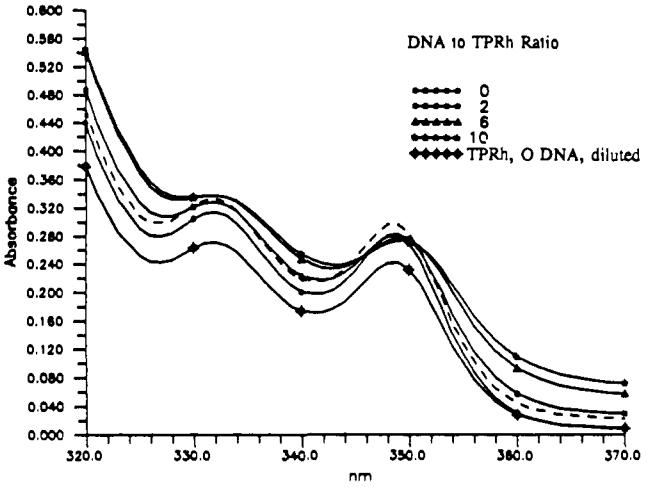

Figure 6. Electronic absorption spectra of TPRh titrated with DNA in a 1 mM phosphate buffer, pH 7, 2 mM NaCl; dashed line = addition spectrum of TPRh and DNA.

Scatchard analysis,[35] in which identical and independent binding sites (one binding site per DNA phosphate) were assumed (an assumption deemed sufficient for our purposes of comparing relative binding constants of the different complexes).[36] Table VI also includes optical enrichment data from circular dichroism analyses of the dialysates (see Figure 5).

Single point experiments were run for the other complexes, and these data (plus the results for cisDCBPR) are summarized in Table VII. The enantioselective association of cisDABPR (with preference for the Λ isomer) at the lower ionic strengths has been calculated using the $\Delta\epsilon$ for the Λ enantiomer of cisDCBPR, since the $\Delta\epsilon$ for the bisaquo complex has not been reported.

Electronic Absorption Spectroscopy. The examination of the electronic absorption spectrum of the rhodium complexes in the presence of DNA is hindered by the fact that the binding is weak at the ionic strength used in the standard photolysis reactions (I = 0.22). Nevertheless, the effect of DNA on the electronic

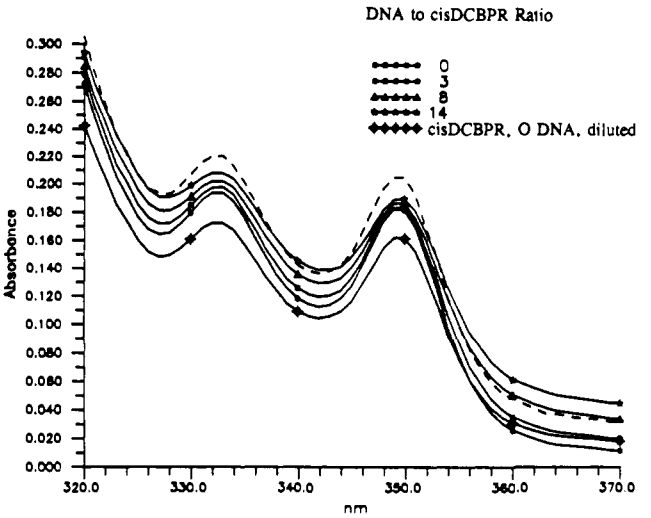

Figure 7. Electronic absorption spectra of cisDCBPR titrated with DNA in a 1 mM phosphate buffer, pH 7, 2 mM NaCl; dashed line = addition spectrum of cisDCBPR and DNA.

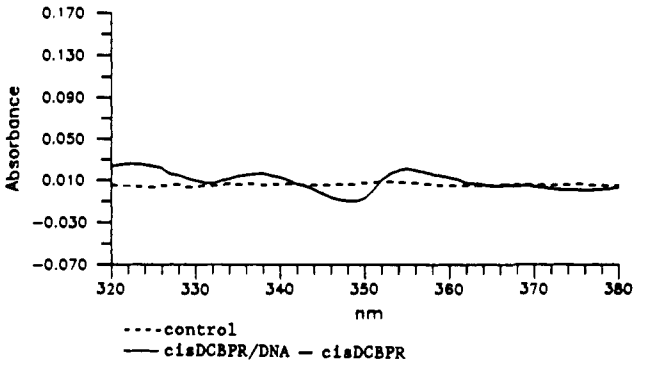

Figure 8. Difference spectrum for admixture of cisDCBPR with DNA in a 1 mM phosphate buffer, pH 7, 2 mM NaCl.

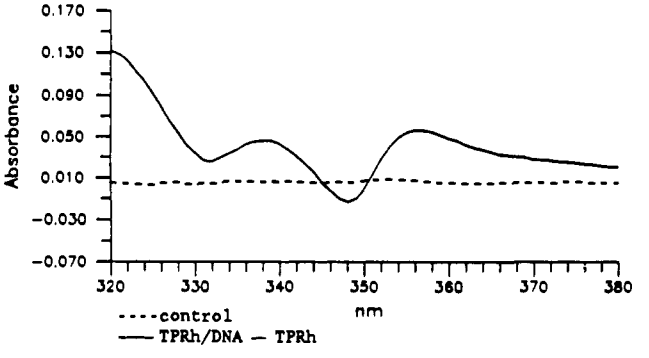

Figure 9. Difference spectrum for admixture of TPRh with DNA in a 1 mM phosphate buffer, pH 7, 2 mM NaCl.

(35) $K = v/[C](n - v)$ where K = the observed binding constant, v = nmols cisDCBPR bound/total nmols DNA(P), [C] = concentration of free ligand (M), and n = number of binding sites per base. This equation reduces to: $K = v/[C]$ if the number of binding sites per DNA(P) is assumed = 1 and v is assumed to be sufficiently small so as to negate the need for subtracting bound sites from the total number of binding sites. Cf. Bloomfield, V. A.; Crothers, D. M.; Tinoco, I. *Physical Chemistry of Nucleic Acids*; Harper & Row: New York, 1974; pp 406–429.

(36) We assumed a value for n, rather than obtaining n from a Scatchard plot, because of the limited number of data points. For intercalating agents, n is often found to be 0.5, explained by the "nearest neighbor exclusion rule";[35] yet lower fractions can be observed, as with tris(phenanthroline)Ru(II), which shows an even greater exclusion of base pairs.[37]

(37) Barton, J. K.; Danishefsky, A. T.; Goldberg, J. M. *J. Am. Chem. Soc.* **1984**, *106*, 2172–2176.

Table VII. Summary of Equilibrium Dialyses Experiments for Metal Polypyridyl Complexes with DNA

	% assoc	K (M^{-1})	% ee	isomer in excess[a]	R^b
		I = 0.22			
cisDCBBR	0	0	0		
cisDCBPR	0	0	0		
cisDABPR	0	0	0		
TPRh	11	2.0E2	2	Δ	1.04
TPRu	22	4.5E2	3	Λ	1.06
		I = 0.022			
cisDCBBR	0	0	0		
cisDCBPR	11	1.5E2	5.5	Δ	1.12
cisDABPR	28	4.7E2	8	Δ	1.17
TPRh	68	2.7E3	13	Δ	1.30
TPRu	67	2.5E3	0		
		I = 0.0042			
cisDCBBR	0	0	0		
cisDCBPR	26	4.3E2	12	Δ	1.26
cisDABPR	53	1.6E3	32	Δ	1.94
TPRh	89	1.1E4	7	Δ	1.15
TPRu	82	6.4E3	0.5	Δ	1.01

[a] Enantiomer observed in the dialysate. [b] Ratio of enantiomers bound to DNA.

transitions of cisDCBPR (and TPRh for comparison) was examined at both low (I = 0.0042) and high ionic strength (I = 0.22). A solution of each complex was titrated with 50–250 μL of concentrated DNA (DNA(P)/drug = 0–16) directly in a 1-cm^2 quartz cell and the spectrum recorded referenced to buffer. The results of these studies are shown in Figures 6 and 7 (the "addition" spectrum shown in these figures is the sum of the spectra for DNA at its highest concentration and for the metal complex, each run separately). The transition at 350 nm for TPRh shows a faint red shift of ca. 2 nm and a very faint diminution in absorption. There is also an increase in absorption in the long wavelength tail as the DNA(P)/Rh ratio is increased. Though there is no corresponding red shift for any of the cisDCBPR maxima, hyperchromicity at long wavelength is also seen for this complex. When this experiment was repeated at higher salt concentrations, the hyperchromic effects observed in the absorption tails were too small to definitively confirm association. Similar observations were made using a DNA(P) to Rh ratio = 10 at low ionic strength and employing "difference spectroscopy" to plot the effects (cf. Figures 8 and 9). Though a small but distinct perturbation is also seen for TPRh at higher ionic strength, the difference spectrum for cisDCBPR is featureless at the higher salt concentration.

Nucleic Acid Melting Curves. Nucleic acid melting studies demonstrate that whether molecules intercalate, minor groove bind, or electrostatically interact with DNA, in each case the DNA helix is stabilized so that the melting temperature increases (i.e., the melting temperature, T_m, is defined as the temperature at which 50% of the double-stranded DNA is converted to single-stranded material.). We utilized poly(dAdT)·poly(dAdT) in these studies since it not only has a sharp and relatively low T_m but also has been used successfully to distinguish between intercalation and electrostatic binding of ruthenium polypyridyl complexes.[32a] We employed a DNA to metal complex ratio (DNA(P) to Rh of 4:1) similar to that used in the photochemical studies; polypyridyl complexes at this ratio have been shown to have a substantial effect on the melting temperature of poly[dAdT)·poly(dAdT).[32a] Two different ionic strengths were employed, 10 mM buffer[32a] and 1 mM buffer plus 2 mM sodium chloride. Our data are presented in Table VIII, with literature data included for purposes of comparison.

C. Isolation and Identification of cisDCBPR/Nucleoside Adducts. Detection of Nucleoside/Rh(phen)$_2$ Adducts from Calf Thymus DNA. Native DNA was photolyzed with cisDCBPR (DNA phosphate to metal ratio = 3.2:1) in phosphate buffer (pH 7) using λ > 330-nm light. After purification by exhaustive dialysis and precipitation, the DNA was resuspended in buffer and treated with DNase I, snake venom phosphodiesterase, and

Table VIII. Melting Transitions for Poly(dAdT)·Poly(dAdT) with Metal Polypyridyl Complexes[a]

	I = 0.022 T_m (°C)	I = 0.0042 T_m (°C)
DNA	43.8 (48)	31.4 (31)
$Rh(phen)_2Cl_2^+$	43.8	32.4
$Rh(phen)_3^{3+}$	>54	>56
$Ru(phen)_3^{2+}$	(53)[b]	(60)[c]
ethidium bromide	>54	>56 (60)
Mg^{2+}	43.7	40.8 (40)

[a] DNA(P) to metal ratio = 4. Values in parentheses are from Kelly et al.[32a] [b] DNA(P) to metal ratio = 20. [c] Value taken from a graph in ref 32a at a DNA(P) to metal ratio of 5.

Table IX. Relative Amount of Nucleosides Detected after Irradiation of cisDCBPR with Calf Thymus DNA and Enzymatic Digestion[a]

	(-) Rh	(+) Rh
dC	0.60	0.59
dG	0.92	0.76
dT	1.00	1.00
dA	0.52	0.54

[a] Data from photolyses of 2.8 mg of calf thymus DNA with 1.8 × 10^{-3} mmol of cisDCBPR for 11 h. Data have been normalized to the thymidine peak area. (-) and (+) Rh refer to DNA irradiated in the absence or presence of the metal complex.

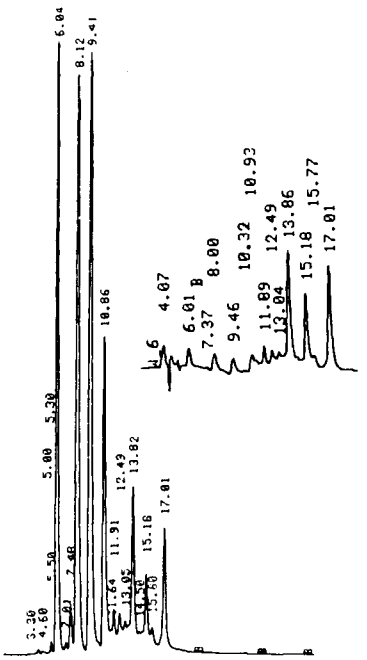

Figure 10. HPLC trace of the DNA enzymatic digest monitored at 280 nm (bottom) and 336 (top).

alkaline phosphatase to yield natural and modified nucleosides. The enzymatic digest was monitored by HPLC at 280 and 336 nm, with the latter allowing for the observation of only those products containing the rhodium bis(phenanthroline) moiety. A typical chromatogram is shown in Figure 10, wherein the unmodified nucleosides can be seen at retention times (min) of 6.04 (dC), 8.12 (dG), 9.41 (dT), and 10.86 (dA). The major nucleoside/rhodium adducts are clearly seen in the 336-nm monitored trace, with retention times of 13.82, 15.18, and 17.01 min (there are at least four additional minor adducts with t_R = 11.9–15.8 min).[38]

(38) There is some evidence that these products are not stable. Reanalysis of this sample after storage at 0 °C for several months showed an enhancement of the 15.8-min peak ("adduct II", see below) relative to the other major peaks. Likewise, the 13.8-min adduct ("adduct I", see below) was partially converted to adduct II upon storage in D_2O at 4 °C in the dark for several weeks. Further studies of the photochemical and thermal interconversion of these adducts are in progress.

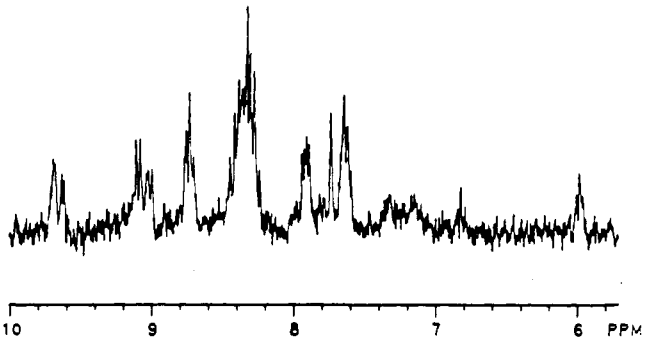

Figure 11. ^{1}H NMR spectrum of adduct I isolated from an enzymatic digest of DNA reacted with cisDCBPR.

Table X. Chemical Shifts for Phenanthroline Hydrogens

H	Phen[a]	TPRh[b]	cis-DCBPR[c]	cis-DABPR[c]	cis-MABPR[d]	adduct I[e]
2	9.93	8.10	10.02	9.61	10.05	9.69
2′					9.52	9.62
3	7.65	7.92	8.44	8.40	8.22	8.32
3′					8.22	8.32
4	8.22	9.05	9.13	9.09	9.11	9.09
4′					9.11	9.01
5	7.61	8.66	8.40	8.38	8.22	8.32
5′					8.22	8.32
6	7.61	8.66	8.26	8.26	8.20	8.32
6′					8.20	8.32
7	8.22	9.05	8.73	8.68	8.72	8.72
7′					8.66	8.72
8	7.65	7.92	7.64	7.58	7.62	7.63
8′					7.56	7.63
9	9.93	8.10	7.86	7.85	7.83	7.91
9′					7.71	7.91

[a] In D_2O, referenced to HDO at 4.76 ppm. [b] In D_2O, cf. ref 39. [c] In D_2O, referenced to DSS. [d] In D_2O, pH 2, referenced to HDO at 4.76 ppm. [e] In D_2O, referenced to acetate at 1.90 ppm.

We were able to estimate the relative reactivity of the metal complex with the DNA nucleotides by quantitation of the unmodified nucleosides in the enzymatic digest. Peak areas from control samples irradiated in the absence of cisDCBPR were compared to the digest from DNA reacted with the metal complex. The results are shown in Table IX, wherein the HPLC areas have been normalized to the thymidine peak in each sample (thymidine was chosen because of the relatively low level of rhodium incorporation into the pyrimidines; cf. Table III). The data clearly show a substantial loss of deoxyguanosine in the enzymatic mixture by comparison with that observed for DNA irradiated in the absence of the complex. By contrast, there is virtually no difference in the dC and dA values under the two sets of conditions.

Isolation and Characterization of Guanosine Adducts: "Adduct I". The major adduct at t_R = 13.8 min (hereafter denoted as "adduct I") was isolated by preparative HPLC and analyzed by ^{1}H NMR (in D_2O, referenced to acetate at 1.90 ppm). The spectrum is shown in Figure 11 and clearly shows the presence of a nucleoside H1′ resonance at δ 5.98, the dG H8 resonance at δ 7.72, and the phenanthroline resonances between δ 7.6 and 9.7. (The deoxyribose protons upfield of δ 4.5 were obscured by a large HDO signal). Integration indicated the presence of one dG ligand in the complex.

Verification of this assignment as a dG adduct was provided by the independent preparation of this adduct by irradiation of cisDCBPR with 2′-deoxyguanosine 5′-monophosphate, followed by treatment with alkaline phosphatase. HPLC analysis of the enzymatic digest gave several peaks visible with 336-nm detection, with adduct I as the major product (cf. top of Figure 12; adduct I has t_R = 13.5 min in this trace). *This product was isolated by HPLC and its ^{1}H NMR spectrum found to be identical with that presented in Figure 11 for the sample isolated from DNA.* A UV absorption spectrum of this sample showed maxima at 272, 336, and 352 nm, typical of rhodium–bis(phenanthroline) complexes.

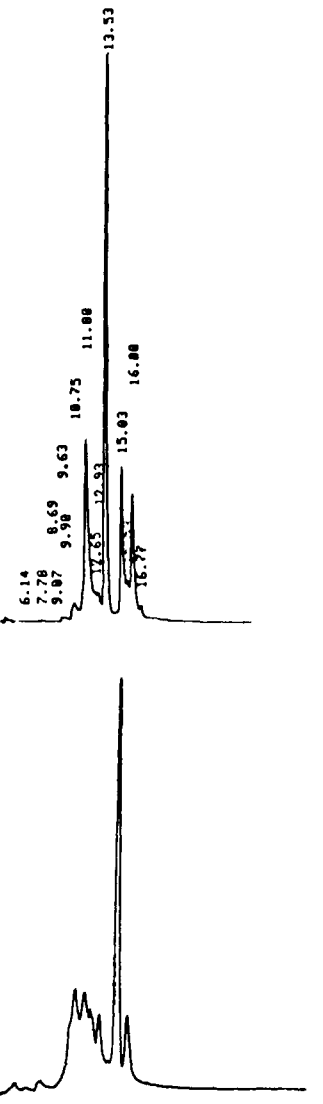

Figure 12. HPLC traces of (top) a dephosphorylated dGMP–cisDCBPR photolysis mixture and (bottom) a dG–cisDCBPR photolysis mixture, both monitored at 336 nm.

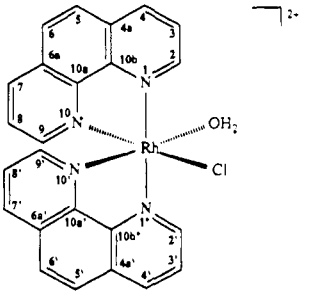

Figure 13. Structure of cisMABPR.

Though we could not obtain sufficient quantities of this adduct to assign a detailed structure, it is useful to compare the chemical shifts of the phenanthroline hydrogens to those of model complexes (cf. Table X). The numbering scheme is illustrated for cis-MABPR (Figure 13). In particular, note that (1) binding of the phenanthroline ligand to the metal (as in TPRh) causes a ca. δ 1 downfield shift except for H2 and H3, where the anisotropic aromatic ring current reduces (H3) or reverses (H2) this effect; (2) the plane of symmetry present in TPRh is broken in cisDCBPR (and cisDABPR), though rotational symmetry still keeps the two

(39) Rehmann, J. P.; Barton, J. K. *Biochemistry* **1990**, *29*, 1701–1709. Rehmann, J. P.; Barton, J. K. *Biochemistry* **1990**, *29*, 1710–1717.

phenanthroline rings magnetically equivalent; (3) the dichlorobisphenanthroline shows small upfield shifts for H5–H9 relative to TPRh but downfield shifts for H2–H4 because of the removal of the third aromatic ring; (4) the chemical shifts for the diaquo complex are quite similar to those of the dichloro complex except for H2, where the change from Cl^- to OH_2 moves the proton upfield by δ 0.4; (5) the rotational symmetry of cisDCBPR and cisDABPR is broken in the chloroaquo complex, most evident at H2 and H2′ and H9 and H9′; the characteristic differential shifts for hydrogens above Rh–Cl vs Rh–OH_2 allows the assignment of H2 in the structure drawn for cisMABPR to the resonance at δ 10.05; and (6) the appearance in adduct I of two resonances for H2 (and H2′) and the concomitant doubling of the H4 resonance are consistent with a $Rh(phen)_2XY$ complex, but the single resonances seen for the other protons indicate X and Y to be very similar ligands; the chemical shifts for the H2 and H2′ hydrogens are consistent with the absence of Cl^- at either site.

Finally, it should be noted that the resonance at δ 7.72 for the guanosine H8 hydrogen is slightly (δ 0.23) upfield from the resonance observed for this hydrogen in free deoxyguanosine, opposite to the marked downfield shift typically observed for metal coordination at N7.[40] This observation is consistent with metalation of the guanosine six-membered ring, analogous to our assignment of structure to adduct II below.[41]

Isolation and Characterization of Guanosine Adducts: "Adduct II". cisDCBPR was also irradiated with 2′-deoxyguanosine in order to eliminate the dephosphorylation step required when working with the nucleotide and to eliminate the possibility of reaction involving the phosphate group. HPLC analysis (cf. bottom of Figure 12) showed the presence of several photoproducts having retention times similar to those observed from photolysis with the nucleotide but with adduct I now as a minor component. The major product (hereafter denoted as "adduct II") corresponded to the peak with t_R = 15 min, identical with the second of the three major adducts observed after enzymatic hydrolysis of metal bound DNA (see above). This was the case when the photolyses were carried out at both pH 7 and pH 9, though there was some enhancement in adduct formation at the higher pH.

Adduct II was isolated and characterized in depth using UV absorption spectroscopy, mass spectrometry, and ^1H as well as ^{13}C NMR spectroscopy. Fast atom bombardment (FAB) analysis of adduct II was recorded in a nitrobenzyl alcohol matrix and gave the highest mass ion at 728 amu, corresponding to a loss of water and two hydrogen atoms from a complex of the formula $Rh(phen)_2dG(H_2O)^{3+}$.[42] The UV absorption spectrum is similar to that observed for adduct I, i.e., transitions are observed at 272, 336, and 352 nm, analogous to those observed for the parent dichloro complex. Treatment of the adduct with acid or base induced minor reversible changes in the spectrum.

^1H NMR spectra were recorded in D_2O and, for a separately and freshly isolated sample, in DMSO-d_6; the data are tabulated in Table XI. Focusing first on the spectrum in D_2O, several features of the data warrant comment: (1) integration of the resonances confirmed the presence of one dG ligand in the adduct; (2) the nature of the phenanthroline region confirms the presence of two nonequivalent cis ligands (see discussion of adduct I above); (3) a comparison of the data for H2 and H2′ with those in Table XII indicates that Cl^- is not one of the ligands; in fact, the unusually high-field position for H2′ is most analogous to TPRh, i.e., there appears to be a particularly effective diamagnetic anisotropic ring current effect on this hydrogen (presumably from the guanosine ring); (4) the proton resonances for H2 and H2′

Table XI. ^1H NMR Spectral Data for Adduct II

H	D_2O[a]	DMSO-d_6[b]
	Nucleoside	
H2″	2.36 (m)	
H2′	2.72 (m)	
H5′,5″	3.74 (m)	
H4′	4.11 (s)	
H3′	4.57 (s)	
H1′	6.22 (t)	6.03 (1 H, t)
C2–NH_2[c]		6.68 (1 H, br s)
C2–NH_2[c]		7.27 (1 H, br s)
H8	7.78 (s)	7.63 (1 H, 2s)
	Rhodium	
OH		9.87 (0.35 H, s)
	Phenanthroline	
H8′	7.61 (dd)	7.79 (2 H, 2dd)
H8	7.65 (dd)	
H9′	7.91 (d)	8.10 (1 H, t)
H9	8.00 (d)	8.22 (1 H, t)
H3′	8.20 (dd)	
H3,6,6′	8.25 (m)	8.44 (6 H, m)
H5′	8.33 (d)	
H5	8.37 (d)	
H2′	8.91 (t)	8.61 (0.5 H, d)
		8.71 (0.5 H, d)
H7,7′	8.73 (2d)	8.89 (2 H, t)
H4′	9.01 (d)	9.18 (2 H, t)
H4	9.20 (d)	
H2	9.60 (t)	9.68 (1 H, d)

[a] Referenced to the acetate methyl protons at 1.90 ppm present in solution from the HPLC buffer. [b] Referenced to TMS at 0.00 ppm. [c] Diesteriotopic hydrogens.

Table XII. ^{13}C NMR Spectral Data for Adduct II[a]

	adduct II	unmodified dG[b]	difference[c]
	Nucleoside Carbons		
C2′	42.28	41.4	+0.9
C5′	65.33	64.3	+1.0
C3′	74.96	73.9	+1.1
C4′	88.01	86.6	+1.4
C1′	90.86	89.8	+1.0
C5	121.18	119.2	+2.0
C8	139.44	140.4	−1.0
C4	152.42	153.9	−1.5
C2	168.38	156.5	+11.9
C6	174.54	161.6	+12.9
	Phenanthroline Carbons[d]		
C8,8′	129.55		
C3,3′	130.43, 130.87		
C5,5′	131.39, 131.56		
C6,6′	131.85		
C4a,4a′[e]	134.77, 134.88		
C6a,6a′[e]	134.95, 135.15		
C7,7′	143.23, 144.26		
C4,4′	144.23, 144.26		
C10a,10′[e]	149.90		
C10b,10b′[e]	150.27, 150.63		
C2,2′	154.73		
C9,9′	154.83, 155.07		

[a] In D_2O, pD 6.0, δ units referenced to the buffer acetate methyl carbon at 25.94 ppm. A resonance seen at 183.6 δ is due to the acetate carbonyl carbon. [b] In D_2O, pD 5.4, referenced to the acetate methyl group of added ammonium acetate at 25.94 ppm. [c] $\delta_{adduct} - \delta_{dG}$, i.e., a + value corresponds to a chemical shift for the adduct which is downfield of unmodified dG. [d] The Phenanthroline carbons were assigned by analogy to the carbon chemical shifts of cisDCBPR, as assigned by a ^1H–^{13}C NMR heteronuclear correlation (HETCOR) experiment (in DMSO-d_6, referenced to solvent at 39.5 ppm): C2 153.05, C9 152.08, C10a 146.93, C10b 146.20, C4 140.76, C7 140.07, C4a 131.55, C6a 131.19, C5 128.51, C6 128.27, C3 127.72, C8 127.20. The assignments for carbons C4a and C6a and carbons C10a and C10b are arbitrary and could be interchanged. [e] The assignments for carbons C4a,4a′ and C6a,6a′ are arbitrary and could be interchanged; the same is true for carbons C10a, 10a′ and C10b, 10b′ (cf. footnote *d* above).

(40) (a) Miller, S. K.; Marzilli, L. G.; *Inorg. Chem.* **1985**, *24*, 2421–2425. (b) Nelson, D. J.; Yeagle, P. L.; Miller, T. L.; Martin, R. B. *Bioinorg. Chem.* **1976**, *5*, 353–358.

(41) This adduct was also found to be the major adduct from the reaction of cisDCBPR with denatured DNA.

(42) We have also observed that the multicharged metal complexes cisDCBPR and cisDABPR give molecular ions with a 1+ charge. Similar observations have been reported in the literature, e.g., the perchlorate complexes of the 2+ species $[M(phen)_3]$, with M = Co, Fe, and Ni, give 1+ molecular ions. Cf. Balasanmugam; Day, R. J.; Hercules, D. M. *Inorg. Chem.* **1985**, *24*, 4477–4483.

are anomalous in that they appear as triplets rather than as the expected doublets; the lack of any reciprocal coupling (for example), in H4 or H4′) confirms that these triplets are in reality two overlapping doublets. The doubling up of these signals is seen again more clearly in the spectrum in DMSO (see below); and (5) the deoxyribose resonances upfield from 4.5 ppm show no change in chemical shift by comparison with unmodified dG, while the nucleoside H8 and H1′ resonances are shifted upfield by 0.17 and 0.07 ppm, respectively, from their positions in the unmodified nucleoside (the former result is again inconsistent with metalation at N7).

The spectrum in DMSO-d_6 is quite revealing in that exchangeable hydrogens can now be seen and the appearance of doubled signals (see H2 and H2′ above) is quite evident (it should be noted that HPLC analysis immediately after acquisition of this spectrum showed no evidence for degradation of the complex). Thus, dG H8, which appears as a singlet in D_2O, is now a closely spaced pair of singlets, the phenanthroline resonances assigned to H9 and H9′ appear as triplets, rather than the commonly observed doublets, and there are now two distinct doublets assignable to H2′. The exocyclic C2–NH_2 protons are split and appear 0.2 and δ 0.8 downfield from that observed for unmodified dG. The resonance at δ 9.87 is assigned to the hydroxide ligand.

Additional NMR Data for Adduct II. Effect of Changes in pH. The lack of a significant change in chemical shift for H8, relative to unmodified nucleoside, argues against metalation at N7 (see above). Confirmation of this conclusion was sought through a study of the effect of pH on H8, i.e., metalation at N7 prevents the otherwise well-known downfield shift caused by protonation of this nitrogen in acidic media.[40a,43] NMR analysis of a freshly isolated sample of the adduct, from pD 6.9 to pD 1.85, using dilute DCl, was found to cause a δ 0.5 downfield shift in H8, as anticipated for N7 protonation.

NOE Analysis. A rotating frame NOESY (ROESY) experiment,[44] using a 400-ms mixing time, gave no evidence for cross peaks between the nucleoside and phenanthroline protons. The expected ROEs were observed between protons of the phenanthroline ring system, such as H8 to H9 and H7, and of the nucleoside, such as H8 to H1′.[45]

^{13}C NMR Spectroscopy. A large volume of cisDCBPR and dG was irradiated and subjected to several lyophilization–centrifugation cycles, after which HPLC and evaporation of the eluent at <30 °C in the dark provided a sufficient sample of adduct II to allow for a ^{13}C NMR spectrum to be recorded at 600 MHz in D_2O at pD 6.0. The chemical shifts are collated in Table XII. Also included in this table are the chemical shifts for unmodified nucleoside and the differences in the chemical shifts between dG and the adduct. One notes that the carbon chemical shifts of the deoxyribose ring are essentially unchanged by metalation of the dG. However, C8 and C4 in the purine ring are shifted δ 1.0 and 1.5 upfield, respectively, relative to unmodified dG, while C5, C2, and C6 are shifted δ 2.0, 11.9, and 12.9 downfield, respectively.

A ^{1}H NMR spectrum of adduct II in D_2O was recorded after acquisition of the carbon spectrum and gave evidence for the presence of two similar species, much as was noted earlier for the ^{1}H NMR spectrum in DMSO. Thus, the spectrum showed a pair of two dG H8 singlets, dG H1 appears as a quartet, rather than as a triplet, and several of the phenanthroline proton resonances are doubled.[46] Nevertheless, there was no evidence of a second species by HPLC.

Structure Assignment for Adduct II. The mass spectrum and ^{1}H and ^{13}C NMR spectra clearly indicate that this adduct has

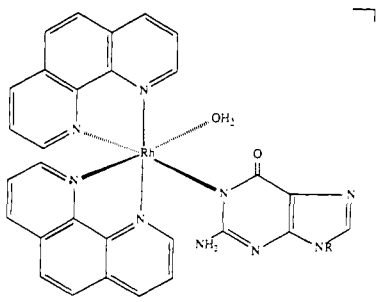

Figure 14. Proposed structure for adduct II.

Table XIII. ^{1}H NMR Spectral Data for Adduct III[a]

	Nucleoside	
H2″	2.57, m	1 H
H2′	2.80, m	1 H
H5′,5″	3.79, m	2 H
H4′	4.18, m	1 H
H3′	4.64, m	1 H
H1′	6.43, t	1 H
H8	8.15, s	1 H
H2	8.24, s	1 H
	Phenanthroline	
H8,8′	7.72, 7.76, 2 dd	2 H
H9′	7.95, d	1 H
H9	8.06, d	1 H
H3′,6,6′	8.35–8.39, m	3 H
H3	8.41, dd	1 H
H5′	8.44, d	1 H
H5	8.48, d	1 H
H7,7′	8.85, 8.84, 2 d	2 H
H4	9.14, d	1 H
H4′	9.19, d	1 H
H2′	9.64, d	1 H
H2	9.76, d	1 H

[a] D_2O, pH 6.0, referenced to DSS at 0.00 ppm.

the structure *cis*-Rh(phen)$_2$dG$(H_2O)^{3+}$. We specifically assign the structure to that shown in Figure 14, with the metal binding site placed at dG N1, for the following reasons. (1) There is no evidence for metalation at N7; H8 is not shifted downfield, as would be expected for metalation at this position,[12,40a,47] nor do we observe the anticipated[40b,48-50] downfield (ca. δ 0.3–0.4) shift from C8 in the ^{13}C spectrum. The pH study, which indicates that N7 is available for protonation, provides further confirmation for this conclusion. (2) Conversely, the very large (δ 12–13) downfield shifts observed for C2 and C6 are consistent with metal coordination at N1 (e.g., Hg(II)CH_3), which is reported to cause downfield shifts of δ 3–5 for these carbons.[48,51] (3) Metalation at N1 would accentuate the magnetic nonequivalence of the diastereotopic C2–NH_2 hydrogens. A particularly intriguing feature of the spectral data is the NMR evidence for the presence of two very similar species in solution. We tentatively ascribe this to the presence of a mixture of adducts containing the hydroxide or aquo group as the second ligand in the pH 5–8 range of these studies.[52a,54] In support of this proposal we note that the phen-

(43) den Hartog, J. H. J.; Salm, M. L.; Reedijk, J. *Inorg. Chem.* **1984**, *23*, 2001–2005.
(44) Kessler, H.; Griesinger, C.; Kerssebaum, R.; Wagner, K.; Ernst, R. R. *J. Am. Chem. Soc.* **1987**, *109*, 607–608; Loschner, T.; Engels, J. W. *Nucleic Acids Res.* **1990**, *18*, 5083–5095.
(45) Wuthrich, K. *NMR of Proteins and Nucleic Acids*; Wiley: New York, 1986; pp 203–214.
(46) The doubling up of the resonances in this spectrum is more evident than was the case for the previous spectrum in D_2O. This may be due to the fact that the earlier spectrum was recorded at pD 8 while the sample used to acquire the ^{13}C spectrum was at pD 6. See below.
(47) Alessio, E.; Xu, Y.; Cauci, S.; Mestroni, G.; Quadrifoglio, F.; Viglino, P.; Marzilli, L. G. *J. Am. Chem. Soc.* **1989**, *111*, 7068–7071.
(48) Buncel, E.; Norris, A. R.; Racz, W. J.; Taylor, S. E. *Inorg. Chem.* **1981**, *20*, 98–103.
(49) Barbarella, G.; Bertuluzza, A.; Morelli, M. A.; Tosi, M. R.; Tugnoli, V. *Gazz. Chim. Ital.* **1988**, *118*, 637–642.
(50) Jenette, K. W.; Lippard, S. J.; Ucko, D. A. *Biochem. Biophys. Acta.* **1975**, *402*, 403–412.
(51) Buchanan, G. W.; Bell, M. J. *Magn. Reson. Chem.* **1986**, *24*, 24463–497.
(52) One might also invoke the slow interconversion of conformational isomers through rotation about the rhodium–dG bond to explain the existence of two very similar species. Hindered rotation about the metal–N7 bond has been observed for square planar complexes with bulky ligands, for example, with Pt, by the presence of two H8 signals in the ^{1}H NMR spectrum of the adduct of (2,2,*N*,*N*-tetramethyl-1,3-propanediammine)Pt(II) and GMP.[53] (b) Lee, L.; Clark, S. F.; Petersen, J. D. *Inorg. Chem.* **1985**, *24*, 3558–3561.

Table XIV. ^{13}C NMR Chemical Shift Data for Adduct III[a]

	adduct III	unmodified dA[b]	difference[c]
	Nucleoside Carbons		
C2′	41.8	41.7	+0.1
C5′	64.3	64.4	−0.1
C3′	73.8	74.0	−0.2
C4′	87.2	87.4	−0.2
C1′	90.2	90.1	+0.1
C5	125.0	121.7	+3.3
C8	142.3	143.0	−0.7
C4	146.7	151.1	−4.4
C2	148.3	155.1	−6.8
C6	163.7	158.3	+5.5
	Phenanthroline Carbons		
C8,8′	129.03, 129.20		
C3,3′	129.74, 130.03		
C5,5′,6,6′	131.04,[d] 131.19, 131.23		
C4a,4a′,6a,6a′	134.26, 134.41, 134.69[d]		
C7,7′	143.35[d]		
C4	143.95		
C4′	144.05		
C10a,10a′,10b,10b′	149.02, 149.26, 149.36, 149.72		
C2,2′	153.32, 155.13		
C9,9′	153.84, 154.76		

[a] D_2O, pH 5.0, referenced to acetate methyl carbon at 25.94 δ. Resonances are also seen for the acetate carbonyl carbon at δ 183.96 and the methanol carbon at δ 51.70. [b] D_2O, pH 6.0, referenced to acetate methyl carbon at δ 25.94. [c] $\delta_{adduct} - \delta_{dA}$, i.e., a + value corresponds to a chemical shift for the adduct which is downfield of unmodified dA. [d] Two carbons.

anthroline hydrogens affected are those which also respond to the replacement of the aquo ligand by chloride, the chemical shift of the hydroxide hydrogen is in the region observed for the bisaquo complex in DMSO, and the pK_as of aquo ligands on rhodium are in the 6–8 range.[52b,55]

Isolation and Characterization of a 2′-Deoxyadenosine Adduct: "Adduct III". Since our studies with polyribonucleic acids indicated that substantial covalent binding occurred with polyriboadenylic acid, we also photolyzed cisDCBPR with 2′-deoxyadenosine. After irradiation of a solution having a nucleoside to metal ratio of 4:1 for 24 h, examination by HPLC indicated the presence of one major potential nucleoside–rhodium photoproduct ("adduct III"). The product was isolated by HPLC, lyophilized, and subjected to spectral characterization.

FAB-MS analysis in a nitrobenzyl alcohol matrix gave a molecular ion of 732.0 corresponding to $[Rh(phen)_2(dA)(H_2O)]^{3+}$ (confirmed by integration of the ^1H NMR spectrum (see below)). The UV absorption spectrum, recorded in H_2O, is identical to that of the deoxyguanosine adducts I and II, with this adduct showing reversible changes in its electronic absorption spectrum upon treatment with acid or base analogous to those of adduct II.

A ^1H NMR spectrum was recorded in D_2O, and the data are presented in Table XIII. The ^1H NMR spectrum was also recorded in DMSO-d_6 using a freshly isolated aliquot of adduct III. The C6–NH_2 exchangeable protons were visible at both δ 6.82 and 7.51, δ 0.06 upfield and δ 0.07 downfield from the chemical shift position in unmodified dA.

The proton resonance of the dA H1′ appears as a triplet at δ 6.43, δ 0.02 downfield from this resonance in unmodified dA. The singlets assigned to dA H8 and H2 (see below) appear δ 0.14 upfield and δ 0.05 downfield from the chemical shift positions for these protons in unmodified dA. No substantial change was noted for the positions of the deoxyribose proton resonances, and, as with adducts I and II, the phenanthroline chemical shifts correspond to those seen for cisMABPR.

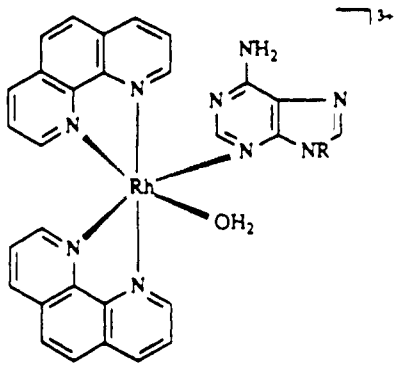

Figure 15. Proposed structure for adduct III.

The carbon NMR data for adduct III are presented in Table XIV, together with the carbon chemical shifts of unmodified dA. Though all the base carbons are shifted relative to unmodified dA, none of these shifts is as large as was seen with adduct II.

The H8 and H2 and C8 and C2 assignments were confirmed using a heteronuclear multiple quantum coherance[56] (HMQC) NMR experiment which allowed the determination of one-bond ^1H–^{13}C connectivities. A heteronuclear multiple-bond correlation[57] (HMBC) analysis was used for the determination of three-bond ^1H–^{13}C connectivities, thus allowing for confirmation of the dA C4, C5, and C6 assignments. A rotating frame NOE analysis[44] of adduct III was also used to confirm the position of H2 downfield of H8. Cross peaks obtained from the NOE analysis showed a dA H1′ cross peak to the most upfield singlet at δ 8.15, assigned to dA H8. No cross peaks were observed between the phenanthroline resonances and those of deoxyadenosine.

Structure Assignment for Adduct III. The combination of mass spectrometry and ^1H NMR confirm that this product is a mono dA adduct with two nonidentical phenanthroline rings. As with adducts I and II we conclude that H_2O is the second ligand on the basis of the chemical shift of the most downfield phenanthroline H2 resonance at δ 9.76. The assignment of the dA binding site is based on the chemical shifts of the deoxyadenosine protons and carbons. As with the dG adducts, neither the carbon nor the proton chemical shifts give evidence for binding to N7, one of the more common binding sites for metals.[58] Metal coordination at this site, such as with Pt(II) or Pt(II), has been reported to cause a slight downfield, rather than upfield, shift for H8[59] and a δ 10 downfield shift for C8.[60] Rather, we find more substantial changes for C5 (δ +3), C6 (δ +6), C2 (δ −7), and C4 (δ −4). These changes and the clearly magnetically nonequivalent NH_2 resonances are consistent with coordination to the six-membered ring. The upfield shifts of C4 and C2 are reminiscent of the upfield shifts observed for carbons α to a protonated pyridine nitrogen[57] and are therefore suggestive of binding at N3. However, there is little precedent in the literature for binding to this hindered and low basicity site. Metal binding at N1 is more common[61] but

(53) Inagaki, K.; Dijt, F. J.; Lempers, E. L. M.; Reedijk, J. *Inorg. Chem.* **1988**, *27*, 382–387. See also: Reily, M. D.; Marzilli, L. G. *J. Am. Chem. Soc.* **1986**, *108*, 6785–6793.

(54) The spectral data available for the third of the major adducts seen upon hydrolysis of metal bound DNA (t_R = 17 min) could not be isolated in an amount sufficient for spectral characterization. Further studies on this adduct are in progress.

(55) We have considered binding at O6 as an alternative to N1 but regard the ^{13}C chemical shifts of the nucleoside as best accommodated by the latter option.

(56) Mueller, L. *J. Am. Chem. Soc.* **1979**, *101*, 4481–4484. Summers, M. F.; Marzilli, L. G.; Bax, A. *J. Am. Chem. Soc.* **1986**, *108*, 4285–4294.

(57) Bax, A.; Summers, M. F. *J. Am. Chem. Soc.* **1986**, *108*, 2093–2094.

(58) Martin, R. B. *Acc. Chem. Res.* **1985**, *18*, 32–38. Uchida, K.; Toyama, A.; Tamura, Y.; Sugimura, M.; Mitsumori, F.; Furukawa, Y.; Takeuchi, H.; Harada, I. *Inorg. Chem.* **1989**, *28*, 2067–2073; Sigel, H. *ACS Symposium Series* **1989**, *402*, 159–204.

(59) Dehand, J.; Jordanov, J. *J. Chem. Soc., Dalton Trans.* **1977**, 1588–1593.

(60) Lim, M. C.; Martin, R. B. *J. Inorg. Nucl. Chem.* **1976**, *38*, 1915–1918.

(61) Pretsch, E.; Clerc, T.; Seibl, J.; Simon, W. *Tables of Spectral Data for the Structure Determination of Organic Compounds*, 2nd ed.; Springer-Verlag: New York, 1981; p C155.

would be expected to cause C2 and C6 to shift upfield and C4 downfield, as has been observed for protonation of purine at this site.[62] We thus tentatively propose the structure shown in Figure 15 for adduct III, recognizing that further confirmation must be forthcoming from, e.g., ^{15}N NMR experiments.

Discussion

Photochemistry. It is clear from the results reported herein that the primary objective of this study has been achieved, i.e., irradiation of cisDCBPR and/or cisDABPR with DNA leads to covalent incorporation of rhodium into the nucleic acid. The UV–vis absorption spectrum of the isolated DNA indicates that the rhodium is incorporated as the $Rh(phen)_2^{3+}$ moiety, with binding of the metal complex to the DNA perturbing the electronic transitions of the nucleic acid but having little affect on the electronic transitions of the metal complex. The spectral data obtained for an adduct isolated from the enzymatic hydrolysis of the metal-bound DNA (adduct I) confirms the presence of a nucleoside ligand (in adduct I, guanosine), but the identification of the other ligand in the metal-bound DNA is not known and no diadduct has been observed.

The rhodium binding levels which can be achieved are quite high, with as much as 1 metal atom per 5 bases having been incorporated (cf. Figure 3). Quantum efficiencies fall in the range of 10^{-3} for both cisDCBPR and cisDABPR (Table V), and consistently higher binding is observed with denatured DNA relative to native DNA. This latter result is not unreasonable, since the DNA bases are more accessible in denatured DNA, but the observation does have some implications for the potential role of intercalation in the initial metal complex/DNA interaction (see below),[63] as does the fact that photolytic incorporation of the complex is enhanced in low ionic strength solutions (Table II). On the other hand, the presence of oxygen appears to have little impact on the level of covalent incorporation of the metal (Table V).

Our observation that the covalent binding of the rhodium complex to DNA occurs enantioselectively is consistent with the literature. The Λ isomer of a similar complex, *cis*-$Ru(phen)_2Cl_2$, has been found to preferentially covalently bind to DNA in the dark,[28] and the recovery of solutions enriched in the Δ isomer from the irradiation of both cisDCBPR and cisDABPR and DNA is indicative of the preferential binding of the Λ enantiomer in our series as well. It is worth noting that the optical enrichment of residual cisDCBPR in these experiments confirms that the dichloride is itself capable of covalent reaction with the DNA, without the necessary intermediacy of aquated photoproducts. One can, of course, speculate as to whether the observed enantioselectivity derives from an enantioselective preassociation of the complexes with the DNA; this point is addressed further below.

Based on our studies with the polyribonucleotides (Table III; see also Table IX), it is clear that the photometalation reaction shows a strong selectivity for the purine nucleotides, particularly guanosine, as has been observed for cisplatin. We were therefore not surprised to find that at least two adducts (adducts I and II) isolated from enzymatically degraded, metalated DNA correspond to products resulting from reaction with dG. What was surprising were the spectroscopic results which strongly argued against metalation of N7, the preferred site for reactions of cisplatin[10-14] and the most common site for transition-metal binding.[58] However, the coordination site for metalation may be expected to be a complex function of the metal (and its charge), the pH of the reaction solution, steric interactions, noncovalent (e.g., intercalative) interactions, mechanism of substitution (associative for cisDDP, dissociative for cisDCBPR), etc. Furthermore, the helical structure of native DNA serves to limit site accessibility by having potential metal coordination sites of deoxyguanosine either along the major groove (dG N7) or the minor groove (dG N3) or positioned to hydrogen bond with cytidine (dG C2–NH_2, C6–O and N1–H). Site accessibility may be particularly important for the rhodium complex, by comparison with cisDDP, since the rhodium complex is larger, pseudooctahedral, and chiral. In fact, that adduct (II) for which we have the greatest amount of spectral data appears to result from the binding of rhodium to N1 (Figure 14), a less common but precedented binding site for metalation.[58]

While one is tempted to assign the initial binding site on DNA to that found in the dG–rhodium adduct, caution is warranted. One cannot lightly assume that the binding site is unaffected by the enzymatic procedure, and we, furthermore, have evidence that adducts I and II may be interconvertible, both thermally and photochemically. *These observations are intriguing because they suggest the possibility that adducts I and II may be diastereomeric isomers resulting from the reaction of the two enantiomeric forms of cisDCBPR with dG.* Finally, though we have isolated and characterized a product from photolysis of cisDCBPR with dA (adduct III), we as yet have not observed an analogous product from enzymatic digestion of metalated DNA.

Noncovalent Interactions of cisDCBPR with DNA. Both the presence of the two planar aromatic phenanthroline ligands and the positive charge on the metal could be expected to facilitate noncovalent interactions between cisDCBPR and DNA, and it is well-known that octahedral metal complexes do associate with DNA.[5,37,64,65] Somewhat to our surpise, however, at the ionic strength typically used in our photolyses our probes give no evidence for association of the rhodium complex with the nucleic acid, whether by an intercalatory mode or by electrostatic interactions. We had no difficulty observing such association with, e.g., TPRu and TPRh (Tables VII and VIII).

In fact, while the interaction of such tris(polypyridyl)–metal complexes with DNA has been extensively studied, the association of metal complexes containing two bidentate aromatic ligands and two inorganic ligands with DNA are less well characterized. Thus, the neutral complex $Ru(phen)_2(CN)_2$ does not appear to intercalate into DNA, even with $I = 0.002$.[32a] By contrast, it has been proposed that $Ru(phen)_2Cl_2$, also a neutral complex but presumably admixed in solution with hydrolyzed, charged products, covalently binds to DNA (in the dark) through prior intercalation.[28]

Experimental parameters, such as ionic strength and the DNA(P) to drug ratio, are known to influence levels of association. Our photochemical experiments were carried out using a standard ratio of DNA(P) to metal of ca. 5:1 in a 100 mM phosphate buffer solution with a relatively high ionic strength of $I = 0.22$, comparable to the physiological ionic strength ($I = 0.16$). The DNA to metal ratio is similar to that used by other researchers, but the ionic strengths employed in the literature are often 0.1–0.05 or lower. The increased *covalent* binding we observed at such lowered ionic strengths (Table II) promoted us to examine noncovalent association with $I = 0.02$–0.0042, and, under the lower ionic strength conditions, both equilibrium dialysis and electronic absorption spectroscopy do indeed give evidence for association. The binding constant is relatively low, however, on the order of 10^2. This is in contrast to the TPRh which has a binding constant with calf thymus DNA of 5000 ± 2000 in 5 mM tris buffer with 50 mM NaCl.[39]

The circular dichroism studies provide additional evidence for association of cisDCBPR at low ionic strengths. Though there is no evidence of enantiomeric enrichment in the dialysate when cisDCBPR is dialyzed against DNA with $I = 0.22$, the dialysate becomes enriched in the Δ isomer as the ionic strength is lowered (Table VII). Two binding modes for metal–tris(polypyridyl) complexes to DNA have been proposed:[8,37,39,64-66] intercalation, wherein the Δ isomer binds preferentially, and a "groove" or "surface" binding, with a preference for the Λ isomer. Our observation of enrichment in the cisDCBPR Δ isomer in solution

(62) Pugmire, R. J.; Grant, D. M. *J. Am. Chem. Soc.* **1971**, *93*, 1880–1887.

(63) It should be noted that native calf thymus DNA is not expected to be completely double stranded, nor is the heat denatured nucleic acid likely to be completely free of base paired regions.

(64) Pyle, A. M.; Rehmann, J. P.; Meshoyrer, R.; Kumar, C. V.; Turro, N. J.; Barton, J. K. *J. Am. Chem. Soc.* **1989**, *111*, 3051–3058.

(65) Barton, J. K. *Pure Appl. Chem.* **1989**, *61*, 563–564.

(66) Kumar, C. V.; Barton, J. K.; Turro, N. J. *J. Am. Chem. Soc.* **1985**, *107*, 5518–5523.

could be taken as evidence for the latter mechanism.[67-69]

It is interesting to speculate as to whether an undetectably low level of preassociation of cisDCBPR and DNA, at the higher ionic strength characteristic of the photolyses, is nevertheless a prerequisite for covalent binding. The evidence in hand does not support such a proposal. Thus, as noted in Table VII, we see no evidence for interaction of DNA with the bipyridyl analog cisDCBBR (a similar observation has been made for $Ru(bpy)_3^{2+}$),[64] and yet we find the quantum efficiencies for binding the bis(bpy) complex to be comparable to those observed for cisDCBPR.[70] Furthermore, we note that the bis(aquo) complex cisDABPR associates with DNA to a greater degree, and with more enantioselectivity, than the dichloride (Table VII) and yet shows no greater quantum efficiency for photolytic covalent binding (Table V). Further data will be needed to resolve this issue.

Summary

The initial objective of these studies has been achieved, i.e., a prototypical system has been developed involving the photolytic covalent binding of a metal complex (cisDCBPR) to DNA using a reactant which is otherwise stable in the dark. The reaction is not dependent on oxygen and proceeds with moderate (ca. 10^{-3}) quantum efficiency. The reaction is enhanced in low ionic strength media, where electrostatic and/or intercalatory association is evident, and occurs with modest enantioselectivity. Two covalent adducts involving deoxyguanosine as a ligand have been isolated from the enzymatic degradation of metalated DNA, one of which is spectroscopically identical with an adduct prepared from the reaction of cisDCBPR with dG. Extensive spectral characterization of the second dG adduct implicates N1 as the point of attachment of Rh to the base. A stable adduct with dA has also been isolated from photolysis of the metal complex with the nucleoside, and a structure has been tentatively assigned.

Further studies to probe the phototoxicity of cisDCBPR with mammalian cells and to extend these observations to less expensive and longer wavelength absorbing complexes are in progress.

Experimental Section

The majority of this work is extensively described in the literature,[1] so only salient information is detailed here.

Materials. Rhodium trichloride hydrate ($RhCl_3 \cdot nH_2O$) was received on loan from Johnson Matthey, Inc. 1,10-Phenanthroline and 2,2'-dipyridyl were purchased from Aldrich Chemical Co. Hydrazinium hydrochloride was from Matheson, Coleman and Bell. The metal complexes *cis*-$Rh(phen)_2Cl_2^+$ (cisDCBPR), *cis*-$Rh(phen)_2Cl(H_2O)^{2+}$ (cisMABPR), *cis*-$Rh(phen)_2(H_2O)_2^{3+}$ (cisDABPR), *cis*-$Rh(bpy)_2Cl_2^+$ (cisDCBPR), and $Rh(phen)_3^{3+}$ (TPRh) were prepared according to literature procedures, with the diaquo complex so prepared utilized for the identification of this cisDCBPR photoproduct. The concentrations of cisDCBPR and cisDABPR were determined spectroscopically using ϵ = 2570 and 2250 M^{-1} cm^{-1} at 351 nm, respectively. $[Ru(phen)_3]Cl_2$, no. 17556, was from Alfa Products, Danvers, MA. Calf thymus DNA (Type I, No D-1501), Poly G (P-4404), Poly A (P-9403), Poly U (P-9528), Poly C (P-4903), 2'-deoxyadenosine 5'-monophosphate (D-6250), 2'-deoxyadenosine (D-7400), 2'-deoxyguanosine 5'-monophosphate (D-9500), bovine pancrease DNase I (D-1126), snake venom phosphodiesterase (Type III) from *Crotalus atrox* (P-6761), bacterial alkaline phosphatase (P-4252), 3-(trimethylsilyl)-1-propanesulfonic acid (DSS), cellulose dialysis sacks (250-9U or 7U), and poly(dAdT)·poly(dAdT) (P-5782) were from Sigma Chemical Co. The concentrations of the polyribonucleotides were determined using the following extinction coefficients: Poly G (ϵ 9.5 × 10^3 M^{-1} cm^{-1} at 254 nm), Poly A (ϵ 10.7 × 10^3 M^{-1} cm^{-1}), Poly C (ϵ 6.3 × 10^3 M^{-1} cm^{-1}), and Poly U (ϵ 9.6 × 10^3 M^{-1} cm^{-1}). 2,2'-Bipyridyl (D21630-5), 99.8, 99.9, and 99.96% D_2O, and d_6-DMSO were from Aldrich. 2'-Deoxyguanosine was from US Biochemicals (14300). HPLC-grade reagents were from Burdick and Jackson Laboratories. All water used was deionized and distilled using a Corning MP-1 water still. The phosphate buffer solutions were prepared volumetrically by combining sodium phosphate mono- and dibasic in the appropriate amount to give a pH = 7.0.

Instrumentation. Photolyses were done in a turntable using a Canrad-Hanovia 450-W Hg lamp (Model 679A-36) encased with a uranium yellow filter transmitting wavelengths greater than 330 nm. Samples were irradiated 6 cm from the light source in cylindrical Pyrex tubes maintained at 12–15 °C with a Neslab Endocal refrigerated circulating bath. At this distance the intensity, through air, was ca. 700 $\mu W/cm^2$, determined using a UVX Radiometer equipped with a UVX-36 sensor. UV absorption spectra were recorded using a Perkin-Elmer Lambda 3B UV–vis spectrophotometer. Unless otherwise specific, spectra were recorded in 1-cm^2 matched quartz cells (Wilmad). Difference spectra were recorded using the Perkin-Elmer spectrophotometer equipped with an arithmetic mode used for spectra subtraction. Quantitation of rhodium was done on a Perkin-Elmer 2380 air/acetylene flame atomic absorption spectrophotometer. A Perkin-Elmer rhodium hollow cathode lamp was used with the instrument set at 343.5 nm, 0.2 slit width, and a gain of 75. Standards were prepared in 10% HCl by diluting a rhodium standard solution (Sigma, R-3129). CD spectra were recorded on a Jasco J-600 spectropolarimeter. The samples were run with maxmium UV absorbance of 1 AU taken on the HP-8451A spectrophotometer.

Samples were freeze-dried using a benchtop Virtis lyophilizer equipped with a Neslab Cryocool (CC-60) cooling unit and vacuum pump. The sample was placed in a Labconco lyophilization flask and frozen with liquid nitrogen prior to drying. The pH of buffer solutions was recorded using a Corning pH meter (476541) calibrated using standard solutions at pH 4, 7, and 10 (Sargent–Welch). The pH of the solutions analyzed by NMR were recorded using an Ingold 6030-3 5-mm microprobe (Wilmad).

Samples were centrifuged using a benchtop Damon/IEC (Model HN-SII) centrifuge at 2000 rpm for 10 min in 15- or 30-mL Corex centrifuge tubes.

NMR Spectroscopy. NMR spectra were obtained either on a General Electric QE-300, a Varian VXR-500, or a Varian VXR-600 spectrometer. Spectra were recorded in D_2O or DMSO-d_6. The pHs of the samples analyzed by NMR spectroscopy were recorded using a Ingold 6030-3 microprobe (Wilmad) standardized at pH 4, 7, and 10 with Sargent-Welch buffer solutions; measurements given are direct meter readings and are uncorrected. The residual HDO resonance was decoupled with presaturation, and ^1H and ^{13}C spectra were referenced internally to the methyl resonance of acetate ($\delta_H = X$ ppm and $\delta_C = y$ ppm).

A ROESY spectrum was acquired on adduct II in D_2O with 4096 complex points in the t_2 dimension and 256 t_1 increments using the States method of phase cycling. The experiment was run on a Varian VXR-500 spectrometer with a mixing time of 400 ms, a recovery period of 3 s, and a 7000-Hz spectral window in both dimensions. The ROESY spectrum of adduct III was acquired with identical parameters except that a 300-ms mixing time and a 4.2-s recovery period were used. The HMQC spectrum was acquired on a Varian VXR-600 using the TPPI method of phase cycling with 1920 points and spectral width of 6500 Hz in the $t_2(^1H)$ dimension and 2000 points and a spectral width of 37709 Hz in the $t_1(^{13}C)$ dimension. Broad-band ^{13}C WALTZ decoupling was applied during the 148-ms acquisition period. Thirty-two transients per FID were collected with a 2-s delay between each scan. The HMBC spectrum was acquired with identical t_1 and t_2 parameters with 96 transients per each FID using a 1-s delay.

Chromatography. HPLC employed a Varian 5000 series chromatograph with ternary capability equipped with a 7125 Rheodyne injection valve, a 0.2-mL injection loop, and a Varian 2050 variable wavelength detector set at 280 or 336 nm. The chromatographs were recorded and processed using a Perkin-Elmer LCI-100 computing integrator. The standard column used in these analyses was a Hamilton PRP-1 analytical (4.6-mm × 25-cm) column (Reno, NV) or a semipreparative column equipped with a guard column containing PRP-1 packing material. Detection was at 280 nm unless otherwise noted. Analysis of free rho-

(67) There is some controversy in this area; it has also been proposed that TPRu only associates through two differently oriented complexes in the major groove. Cf. Hiort, C.; Norden, B.; Rodger, A. J. *J. Am. Chem. Soc.* **1990**, *112*, 1971–1982. Recent results indicate nonintercalative binding of TPRu to the minor groove of an oligonucleotide. Cf. Eriksson, M.; Leijon, M.; Hiort, C.; Nordén, B.; Gräslund, A. *J. Am. Chem. Soc.* **1992**, *114*, 4933–4934.

(68) A further examination of Table VII indicates that this conclusion must be taken with some caution. We have found that at I = 0.22 there is a preferential association of the Λ enantiomer of TPRh (which has a 3+ charge) but of the Δ enantiomer of TPRu (which has a 2+ charge). Furthermore, the preferential association of the TPRu Δ enantiomer is reversed at I = 0.0042, where there is a faint preference for the Λ isomer. This change in enantiomeric preference as a function of ionic strength (and of the GC content of the DNA) has been previously noted.[8] A more recent study, utilizing NMR spectroscopy, led to the conclusion that higher charged complexes favor surface association relative to intercalation.[59]

(69) One might have therefore anticipated that cisDCBPR would have a minimal effect on the melting transition of poly(dAdT)·poly(dAdT) by comparison with ethidium bromide (Table VIII). We are surprised, however, that even Mg^{2+} has a greater effect on the melting transition than the metal complex; the implication is that association of the complex is, e.g., GC specific, and further studies on this point are in progress.

(70) Torregrosa, S. Unpublished results.

dium complexes and nucleoside adducts utilized a gradient from 100% A to 100% B in 20 min at a flow rate of 1.5 mL/min, 100% B for 10 min at 1.5 mL/min, and then a gradient to 100% A in 15 min at a flow rate of 0.5 mL/min. (A = 80% 0.1 M ammonium acetate, pH 7, 20% B, and B = 60% methanol, 20% acetonitrile, 20% 0.1 M ammonium acetate, pH 7.) Products were isolated using a gradient eluent system consisting of 100% A to 100% B in 20 min at a flow rate of 1.5 mL/min. Sephadex chromatography loading a redissolved sample of metalated DNA in 0.5 mL phosphate buffer onto an 11-mm diameter column containing 32 mL wet volume of Sephadex (Sephadex G-25-150, Sigma Chemical Co.) with a bead size (excluding molecules of average molecular weight) greater than 5000. The DNA was eluted with 0.1 M phosphate buffer (pH 7), and 3-mL fractions were collected and analyzed by UV-vis absorption spectroscopy.

Photolyses with DNA. The DNA/rhodium photolysis mixtures were immediately dialyzed against 400 mL of 0.005 M Tris buffer at 4 °C in the dark. The dialysate was changed 3–4 times over a 3-day period. After dialysis the DNA was precipitated using 0.1 × volume of 2 M NaCl and 2 × volume of ethanol. The samples were then stored at 0 °C for at least 12 h and then centrifuged. The ethanol/NaCl supernatant was discarded and the DNA was kept at room temperature for 0.5–1 h to remove residual ethanol. The DNA was resuspended in either 0.05 M Tris buffer (pH 7) (if the samples were to be reprecipitated) or in distilled water and kept at room temperature until the DNA was dissolved (1–2 days).

Typically, the amount of DNA remaining after reaction with the metal complex was determined by colorimetric analysis using the "Burton assay".[71] Rhodium quantitation was done by atomic absorption in which an aliquot of resuspended DNA was treated with concentrated HCl and H_2O to make a 10% solution and heated to 70 °C for 20–30 min. Each DNA/rhodium sample was analyzed in duplicate using the Burton assay and by atomic absorption.

Quantum efficiencies for the covalent binding of rhodium to the DNA were determined at 308 nm using a 1-cm^2 quartz cell, with the average laser intensity measured by a Scientech #362 power meter in units of watts (W = J/s). Deoxygenated samples were bubbled with argon for 30 min prior to irradiation. Both aerated and deoxygenated samples were sealed with a rubber septum prior to photolysis and mixed manually during irradiation. The samples were irradiated with a Lambda Physik EMG 50 XeCl excimer laser at 30 kV and 28 Hz at an average laser intensity of 0.137 W for 4 min with manual mixing every 30 s. Only 1 cm^2 of the 2.6-cm^2 beam was used. The intensity per pulse was 4.9 mJ/pulse, and the pulse width was 10 ns.

Preparation and Isolation of Adduct I from DNA. Calf thymus DNA was prepared by dissolving the DNA overnight in 0.1 M phosphate buffer (pH 7). The concentration of DNA was determined by UV absorption spectroscopy using a conversion factor of 21 absorbance units/mg of DNA. Fifteen milliliters of DNA (1.7 mg/mL) was irradiated with 5 mL of cisDCBPR (4.9 mM) for 2 h in several Pyrex tubes. After photolysis the DNA samples were combined and exhaustively dialyzed against 5 mM Tris buffer, precipitated with 2-volume 95% ethanol and 0.1-volume 2 M NaCl, and stored at 0 °C overnight. After centrifugation, the DNA pellet was dissolved in 10 mM Tris buffer (pH 7.2) (10 mL) followed by the addition of 100 mM $MgCl_2$ and DNase I. The sample was incubated overnight, brought to pH 9 by the addition of 100 mM Tris buffer (pH 9), and treated with snake venom phosphodiesterase (SVPD) followed by incubation for 12 h. A second aliquot of SVPD was added, incubated 12 h, and finally treated with alkaline phosphatase and incubated for an additional 6–12 h. All incubations were done at 37 °C. The sample was filtered, reduced in volume with nitrogen (ca. 24–48 h in the dark at room temperature), and stored at 0 °C for several weeks prior to analysis by HPLC. Adduct I was isolated by HPLC, concentrated with nitrogen, treated with D_2O, lyophilized, and dissolved in D_2O for analysis by ^{1}H NMR. Though in general the typical volume of enzyme used in each step was 0.1 mL for a solution containing 2–4 mg of DNA in 2 mL of Tris buffer and 0.1 mL of 100 mM $MgCl_2$, due to the larger amount of DNA used in the preparation of adduct I, the amount of each enzyme was increased in this study. Analysis of the enzymatic digest by HPLC was used to determine the enzyme reactivity by the observation of the four free nucleosides present in solution. Enzymatic digestion of large amounts of DNA using this procedure was found to be more successful if the DNA was separated into several smaller volumes rather than by directly treating one large volume. During the enzymatic procedure the DNA was kept in the dark; however, all other manipulations exposed the DNA to room light.

Preparation and Isolation of Adduct I from 2′-Deoxyguanosine 5-Monophosphate. Ten milliliters of dGMP (7.6 mM) was mixed with 10 mL of cisDCBPR (2 mM) in 0.01 M Tris buffer (pH 8.4), and the solution was irradiated in Pyrex tubes for 140 min. The sample was concentrated to ca. 2 mL with nitrogen in the dark at room temperature, treated with 0.1 mL of alkaline phosphatase, and incubated overnight at 37 °C. The sample was reduced in volume with nitrogen, filtered, further reduced in volume to ca. 0.5 mL, and stored at 0 °C several weeks prior to HPLC analysis. Isolation of adduct I for analysis by NMR spectroscopy. UV–vis spectroscopy, and FAB-MS analysis was done at room temperature and subjected to room light by collecting fresh aliquots from the enzymatic mixture as needed. Each sample was immediately frozen and lyophilized to dryness. Due to the presence of the organic eluent the volume was divided into smaller aliquots for complete drying. The sample of adduct I was treated with D_2O and lyophilized two times prior to acquisition of the NMR spectrum.

Preparation and Isolation of Adduct II from 2′-Deoxyguanosine. The samples used for the ^{1}H NMR and UV–vis absorption spectroscopy, 2D NMR, and FAB-MS analysis were prepared by photolyzing 10 mL of dG (9.2 mM) with 10 mL of cisDCBPR (2.2 mM) in 0.1 M Tris buffer (pH 7) for 24 h. After irradiation the solution was concentrated to ca. 2 mL at room temperature in the dark with nitrogen. The mixture was stored at 0 °C until use. Adduct II was isolated by HPLC, dried by lyophilization, and dissolved in D_2O for NMR analysis. Freshly isolated samples of adduct II were used for the NMR spectra in D_2O and DMSO-d_6, UV–vis spectroscopy, 2D NMR, and FAB-MS analysis. The larger amount of adduct necessary to obtain the ^{13}C NMR spectrum was prepared by photolyzing 200 mL of dG (10 mM) with 200 mL of cisDCBPR (2 mM) in several Pyrex tubes containing ca. 35 mL for 21 h. After irradiation the volume was concentrated to ca. 10 mL by several lyophilization–centrifugation cycles. dG precipitated from solution, and the photolysis solution was decanted from the unreacted starting material. The solution was stored at 0 °C prior to HPLC analysis. Numerous fractions of adduct II were collected, and the large volume of eluent was removed under vacuum at <30 °C. The concentrated sample was dissolved in water and lyophilized.

Preparation and Isolation of Adduct III from 2′-Deoxyadenosine. Twenty millimolar deoxyadenosine (150 mL) was mixed with 5 mM cisDCBPR (150 mL) in 0.05 M Tris buffer (pH 7.2). The sample was irradiated for 24 h and concentrated to ca. 5 mL by repeated lyophilization–centrifugation cycles to remove unreacted dA. The mixture was stored at 0 °C for several weeks prior to HPLC analysis. Small volumes of HPLC eluent (<10 mL) containing adduct III were dried by lyophilization, and larger volumes were dried under vacuum at <30 °C, followed by redissolution and lyophilization. The residue was treated with 99.8% D_2O, lyophilized, and finally redissolved in 99.96% D_2O for analysis by ^{13}C NMR.

Acknowledgment. We are grateful to Dr. D. Carlson for helpful advice regarding the NMR spectroscopy, Professors E. Grant, T. Zwier, and C. Kubiak for use of their laser equipment, and Professors J. Grutzner, D. McMillin, and M. Bina for helpful discussions. Partial support by the National Institutes of Health and a National Institutes of Health National Research Service Award 5T32CA09634 from the Purdue Cancer Center to M.A.B. is gratefully acknowledged.

Supplementary Material Available: S1, ^{1}H NMR spectrum of adduct II, formed from photolysis of cisDCBPR with dG, in D_2O; S2, ^{1}H NMR spectrum of adduct II, formed from photolysis of cisDCBPR with dG, in DMSO-d_6; and S3, ^{13}C spectrum of adduct II in D_2O (3 pages). Ordering information is given on any current masthead page.

(71) Waterborg, J. H.; Matthews, H. R. *Methods in Molecular Biology. Nucleic Acids*; Humana Press: New Jersey, 1984; Vol. 2, pp 1–3.